Gravitational Waves and Binary Black Holes

Thibault Damour
Institut des Hautes Etudes Scientifiques
35 route de Chartres
91440 Bures sur Yvette, France

Abstract. The theoretical aspects of the gravitational motion and radiation of binary black hole systems are reviewed. Several of these theoretical aspects (high-order post-Newtonian equations of motion, high-order post-Newtonian gravitational-wave emission formulas, Effective-One-Body formalism, Numerical-Relativity simulations) have played a significant role in allowing one to compute the 250 000 gravitational-wave templates that were used for searching and analyzing the first gravitational-wave events from coalescing binary black holes recently reported by the LIGO-Virgo collaboration.

1 Introduction

On February 11, 2016 the LIGO-Virgo collaboration announced [1] the quasi-simultaneous observation by the two LIGO interferometers, on September 14, 2015, of the first Gravitational Wave (GW) event, called GW150914. To set the stage, we show in Figure 1 the raw interferometric data of the event GW150914, transcribed in terms of their equivalent dimensionless GW strain amplitude $h^{\rm obs}(t)$ (Hanford raw data on the left, and Livingston raw data on the right).

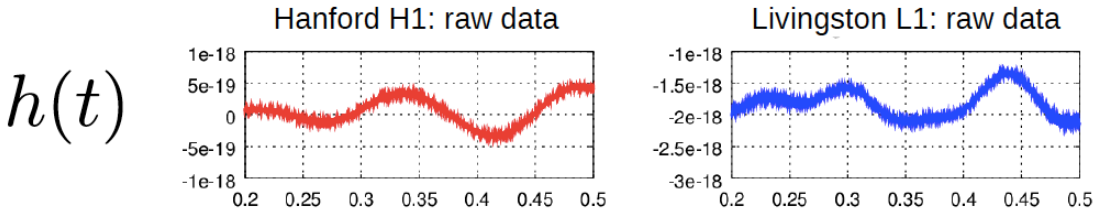

Figure 1: LIGO raw data for GW150914; taken from the talk of Eric Chassande-Mottin (member of the LIGO-Virgo collaboration) given at the April 5, 2016 public conference on "Gravitational Waves and Coalescing Black Holes" (Académie des Sciences, Paris, France).

The important point conveyed by these plots is that the observed signal $h^{\rm obs}(t)$ (which contains both the noise and the putative real GW signal) is randomly fluctuating by $\pm 5 \times 10^{-19}$ over time scales of ~ 0.1 sec, i.e. time scales shorter than the observable duration (~ 0.2 sec) of the coalescence signal. Such a fluctuation level is 500 times larger than the maximum amplitude of the GW coalescence signal due to GW150914, which is $h^{\rm signal}_{\rm max} \simeq 1 \times 10^{-21}$. In other words, the observed (equivalent)

GW amplitude $h^{\rm obs}(t)$ is totally dominated by the colored, broadband noise, $n(t)$, of the detectors:

$$h^{\rm obs}(t) = n(t) + h^{\rm signal}(t) \tag{1}$$

with $|n(t)| \sim 5 \times 10^{-19} \gg |h^{\rm signal}(t)|$.

Methods for detecting the presence of the small signal $h^{\rm signal}(t)$ in $h^{\rm obs}(t)$ have therefore been crucial to the interpretation of the LIGO data. The data analysis, performed by the LIGO-Virgo collaboration, of the raw LIGO data makes use of several methods (generic transient search, matched-filter search) and is done in several stages (online, offline). We refer to the contribution of Eric Chassande-Mottin for a detailed discussion of the various data analysis pipelines. Here we shall focus on the role played by the multi-year theoretical work on the motion and radiation of compact binary systems, and notably on binary black hole (BBH) systems. Indeed, as we shall explain, this work led, more than 10 years before the first detection, to precise predictions for the GW signal $h^{\rm signal}(t)$ emitted by inspiralling and coalescing BBH systems. These predictions have played an important role in defining a large bank of "template" signal waveforms $h^{\rm signal}(t; p_i)$, depending on several parameters p_i, that have been used, via a Matched Filtering technique, both to search for and to physically interpret, GW coalescence signals hidden in the raw LIGO data. To date, the observation of three BBH GW coalescence events have been reported by the LIGO-Virgo collaboration [1, 2]: GW150914, GW151226 and (with a lower confidence level) LVT151012. A theory-based bank of 250 000 template waveforms has been crucially used both to extract from the noise, and to interpret (in terms of the masses and spins of inspiralling and coalescing black holes), these three events. We note in passing that, while the first event GW150914 was loud enough to have been initially identified by an online generic transient search (using a time-frequency-analysis), the other, weaker events were only identified by a matched-filter search (GW151226 having been first identified by an online matched-filter search, and the candidate event LVT151012 having been found in an offline matched-filter analysis).

2 Early contributions to the theory of the gravitational motion and radiation of compact binary systems

Before explaining the rather recent theoretical work that led to precise predictions for the form of the GW signals emitted by coalescing BBHs (which are the only compact binary systems observed so far), we wish to briefly summarize the early history of the theory of the motion and radiation of compact binary systems. [The expression "compact binary systems" refers to systems made either of two black holes, two neutron stars, or one black hole and one neutron star. Most of the recent theoretical work applies to all these systems, though the BBH case is special in that it is the only one for which the theory has been able to accurately predict the full GW signal, from the early inspiralling phase, up until the merger and the post-merger "ringdown".]

2.1 Early contributions to the theory of the gravitational motion of binary systems (in brief)

Einstein (and Droste) introduced around 1912-1916 the useful approximation method called *post-Newtonian* (PN). This is an expansion in $1/c^2$, which gathers, at each or-

der, "slow-motion" relativistic corrections proportional to v^2/c^2, and "weak-gravitational-field" corrections proportional to $GM/(rc^2)$. The PN expansion is a quite efficient approximation scheme which has kept its usefulness over many years (after many theoretical improvements to cure some of its defects). The first post-Newtonian (1PN) approximation to the dynamics of a binary system has been first correctly derived in a famous 1938 paper by Einstein-Infeld-Hoffmann [3]. [An equivalent result was already contained in a 1917 paper by Lorentz-Droste [4], which remained ignored in the literature].

2.2 Early contributions to the theory of the gravitational radiation of binary systems (in brief):

In 1918 Einstein [5] obtained the structure of weak, plane gravitational waves, and derived –modulo a factor 2– the leading-order (LO) emission of GWs from a *non-self-gravitating* source. He found that the LO radiation was quadrupolar in nature, and determined by the second time derivative of the mass quadrupole of the source. More precisely, his results were equivalent to saying that, in a certain coordinate system, the metric perturbation emitted by a general non-self-gravitating source could be written, far from the system (at a point $\mathbf{x} = r\,\mathbf{n}$, with $\mathbf{n}^2 = 1$, in the wave zone), as

$$h_{ij}^{\rm quad}(t,\mathbf{x}) \approx \frac{2G}{c^4 r}\left[\frac{d^2 I_{ij}(t-r/c)}{dt^2}\right]^{TT} \tag{2}$$

where the superscript TT denotes a transverse-traceless projection on the plane orthogonal to the radial direction $n^i = x^i/r$, i.e.

$$A_{ij}^{TT} \equiv \left(P_{ii'}(\mathbf{n})P_{jj'}(\mathbf{n}) - \frac{1}{2}P_{ij}(\mathbf{n})P_{i'j'}(\mathbf{n})\right)A_{i'j'} \tag{3}$$

where $P_{ij}(\mathbf{n}) \equiv \delta_{ij} - n_i n_j$. [We use Einstein's summation convention on repeated indices, and spatial indices $i, j, \ldots = 1, 2, 3$ are raised and lowered by the Euclidean metric $\delta_{ij} = \mathrm{diag}(1,1,1)$, so that, for instance $n_i = n^i$ and $\delta_{ij} = \delta^i_j$.]

To LO, the symmetric trace-free (STF) spatial tensor I_{ij} entering Eq. (2) is the Newtonian mass quadrupole of the source

$$I_{ij}(t) \approx \int_{\rm source} d^3x\,\rho(t,\mathbf{x})\left(x^i x^j - \frac{1}{3}\mathbf{x}^2\delta_{ij}\right) \tag{4}$$

where $\rho(\mathbf{x})$ is the Newtonian mass density of the source.

The quadrupole-emission formula of Einstein was generalized to *self-gravitating* sources (such as binary systems) by Landau and Lifshitz [6] in 1941 (as well as by Fock [7] in 1955). These authors found that, though one cannot neglect, when evaluating the gravitational emission of a binary system, the nonlinear gravitational stresses linked to the self-gravity effects within the source (i.e. the spatial stresses T^{ij} of the material source must be completed by additional contributions t_g^{ij} generated by the nonlinear structure of Einstein's equations), the final result for the emitted waveform can still be written in the form (2) with a quadrupole moment still approximately given by the Newtonian expression (4).

Applying this Einstein-Landau-Lifshitz quadrupole-emission formula to the case of a binary system [with masses m_1, m_2 located at positions $\mathbf{x}_1(t)$, $\mathbf{x}_2(t)$] predicts

that the GW emitted by a binary system is, to LO, given by Eq. (2) with a LO quadrupole moment given by

$$I_{ij}(t) \approx m_1 \left(x_1^i x_1^j - \frac{1}{3} \mathbf{x}_1{}^2 \delta_{ij} \right) + m_2 \left(x_2^i x_2^j - \frac{1}{3} \mathbf{x}_2{}^2 \delta_{ij} \right) \tag{5}$$

In the center-of-mass frame of the binary system, the LO quadrupole moment reads

$$I_{ij}(t) \approx \mu \left(x_{12}^i x_{12}^j - \frac{1}{3} \mathbf{x}_{12}{}^2 \delta_{ij} \right) \tag{6}$$

where

$$\mu \equiv \frac{m_1 m_2}{m_1 + m_2} \tag{7}$$

is the reduced mass of the binary system, and where $\mathbf{x}_{12} \equiv \mathbf{x}_1 - \mathbf{x}_2$ is the relative position.

In addition, as early as 1918, Einstein [5] evaluated the instantaneous flux of energy emitted (at a given retarded time $u \approx t_{\rm field} - r/c$, and over a sphere at infinity) by the source in the form of GWs, and found –modulo a factor 2 which was later corrected by Eddington– that it was given by the following quadratic expression in the third time-derivative of the (radiative) quadrupole moment $I_{ij}(t)$ entering the waveform (2):

$$F^E_{\rm GW}(u) \approx \frac{G}{5c^5} \left[\frac{d^3 I_{ij}(t)}{dt^3} \frac{d^3 I_{ij}(t)}{dt^3} \right]_{t=u} \tag{8}$$

Inserting in the LO "flux quadrupole formula" (8) the LO expression of the quadrupole moment of a binary system, Eqs. (5), (6), and using, at LO, the Newtonian equations of motion to evaluate the third time-derivative of $I_{ij}(t)$ then yields an explicit expression for the instantaneous GW flux emitted by a binary system. The latter expression simplifies in the case where the two bodies move along circular orbits, and yields

$$F^{E\rm circ}_{\rm GW} \approx \frac{32 G^4}{5c^5} \frac{\mu^2 M^3}{r_{12}^5} \tag{9}$$

where

$$M \equiv m_1 + m_2 \tag{10}$$

denotes the total mass of the binary system.

Requiring that the loss of energy in the form of a GW flux at infinity is balanced by corresponding secular loss of the energy of the binary system

$$\frac{dE_{\rm system}}{dt} = -F^E_{\rm GW} \tag{11}$$

and using the LO (Newtonian) value for the binding energy of a circular binary system, namely

$$E^{\rm circ}_{\rm system} \approx -\frac{1}{2} \frac{G m_1 m_2}{r_{12}} \tag{12}$$

yields the following ODE [given as an exercize in Landau-Lifshitz (1941) [6]] for the secular evolution of the relative distance $r_{12}(t)$ of the binary system

$$\frac{dr_{12}}{dt} \approx -\frac{64 G^3}{5c^5} \frac{\mu M^2}{r_{12}^3} \tag{13}$$

or, equivalently,

$$\frac{dr_{12}^4}{dt} \approx -\frac{256G^3\mu M^2}{5c^5} \tag{14}$$

whose solution is

$$r_{12}^4(t) \approx r_{12}^4(0) - \frac{256G^3\mu M^2}{5c^5}\, t = r_{12}^4(0)\left(1 - \frac{t}{t_c}\right) \tag{15}$$

where

$$t_c = \frac{5c^5 r_{12}^4(0)}{256G^3\mu M^2} \tag{16}$$

Note that t_c has the physical meaning of the *time of coalescence* of two point masses, namely the time at which, formally, the relative distance $r_{12}(t) \propto (1-t/t_c)^{\frac{1}{4}}$ vanishes. For comparable masses, $m_1 \sim m_2$, this coalescence time (when evaluated at any time t_0) is of order

$$t_c \sim \frac{P_0}{(v_0/c)^5} \tag{17}$$

where P_0 and v_0 are, respectively, the orbital period and the orbital velocity, evaluated at time t_0.

In a visionary paper of 1963, Freeman Dyson [8] was apparently the first to grasp the most important consequence of this text-book exercize: namely, the fact that GW radiation reaction necessarily drives binary systems closer and closer until the two bodies coalesce in a violent event that will emit an intense burst of GWs. He realized that the GW signal emitted just before and during such a coalescence event will be most important for binary systems made of compact objects. [For objects having larger radii R_1, R_2, the coalescence (which actually takes place when $r_{12} \approx R_1 + R_2$) occurs for a larger relative distance, corresponding to a smaller relative velocity, and a weaker GW signal.] In his paper (written *before* the discovery of pulsars, i.e. at a moment where most people did not take seriously the idea of "neutron stars"), Dyson explicitly considered the case of a an inspiralling binary system of *two neutron stars*, whose inspiral is driven by the energy loss into GWs, and emphasized the potential importance of such coalescence events as GW sources. To quote Dyson:

"According to (11) [the Einstein-Landau-Lifshitz quadrupole formula], the loss of energy by gravitational radiation will bring the two stars closer with ever-increasing speed, until in the last second of their lives they plunge together and release a gravitational flash at a frequency of about 200 cycles and of unimaginable intensity. [...] It would seem worthwhile to maintain a watch for events of this kind, using Weber's equipment or some suitable modification of it."

This vision of Dyson is illustrated in Fig. 2 and Fig. 3. More precisely, Fig. 2 sketches the evolution, Eq. (15), of the relative distance between the two neutron stars (which formally ends up at $r_{12}(t_c) = 0$), while Fig. 3 sketches the corresponding emitted gravitational wave amplitude (estimated by the "quadrupole formula"), which formally ends up as a singular (infinite-amplitude, infinite frequency) oscillatory signal $h(t) \simeq c_1(t_c - t)^{-1/4}\cos(c_2(t_c - t)^{5/8} + c_3)$.

LIGO transformed this theoretical vision of Dyson into reality (for the case of binary black holes; binary neutron star coalescences are still to be detected). Note

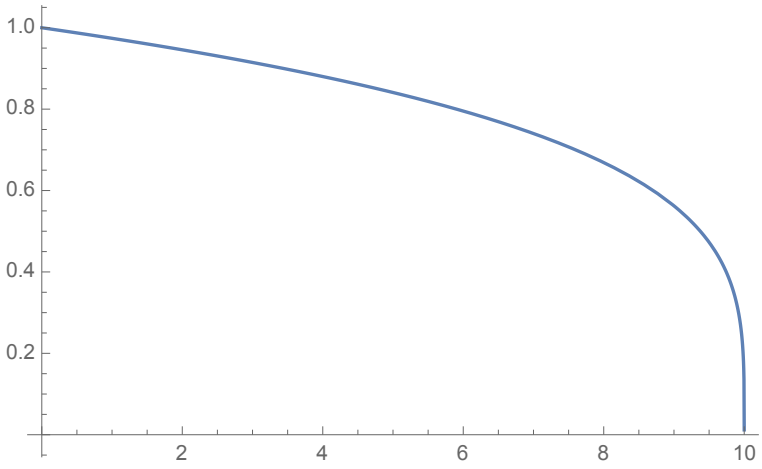

Figure 2: Secular decrease (formally until coalescence: $r_{12}(t_c) = 0$) of the distance $r_{12}(t)$ between the two members of a compact binary, as computed from the leading-order (quadrupole) formula.

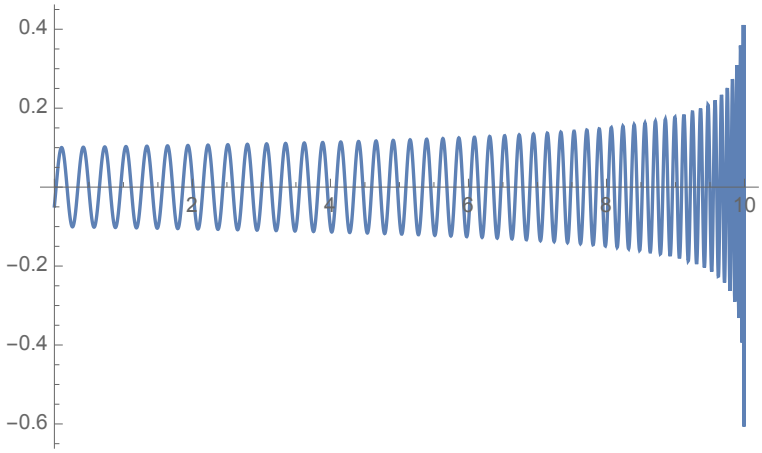

Figure 3: Gravitational wave signal emitted by a coalescing compact binary, as estimated from the leading-order theoretical estimate (quadrupole-formula)

in passing that Dyson's work had been motivated by the pioneering experimental vision (dating from about 1955, when Dyson invited Weber to stay at the Institute for Advanced Study in Princeton) of Joseph Weber that GWs passing on Earth generate observable effects that can, in principle, be detected by a sufficiently sensitive apparatus.

The case of *circular* motions considered by Landau-Lifshitz and Dyson might seem to be generically too special. Peters [9] extended the LO (quadrupolar) energy-loss computation of Einstein (1918) to the computation of the (LO, quadrupolar) loss of *angular momentum*, say $F^{J^i}_{\rm GW}$, of a binary system. Requiring that the GW losses of energy and angular momentum are both balanced by corresponding secular losses of the energy and angular momentum of the binary system,

$$\frac{dE_{\rm system}}{dt} = -\langle F^{E}_{\rm GW}\rangle \tag{18}$$

$$\frac{dJ^i_{\rm system}}{dt} = -\langle F^{J^i}_{\rm GW}\rangle \tag{19}$$

(where $\langle\cdots\rangle$ denotes a time-average over orbital period) he found that a binary system moving on an *eccentric* orbit would *efficiently circularize*. More precisely, expressing, at LO, $E_{\rm system}$, and $J_{\rm system} = J^z_{\rm system}$ in terms of the Newtonian semi-major axis, a, and eccentricity, e, of the Keplerian relative orbit, namely

$$E_{\rm system} \approx -\frac{G\mu M}{2a}\,;\; J_{\rm system} \approx \mu M\sqrt{\frac{Ga(1-e^2)}{M}} \tag{20}$$

and using the LO values of the averaged GW fluxes of energy [10] and angular momentum [9] from eccentric Keplerian binary orbits, namely

$$\langle F^{E}_{\rm GW}\rangle \approx \frac{32G^4}{5c^5}\frac{\mu^2M^3}{a^5}\frac{1+\frac{73}{24}e^2+\frac{37}{96}e^4}{(1-e^2)^{\frac{7}{2}}}\,, \tag{21}$$

$$\langle F^{J}_{\rm GW}\rangle \approx \frac{32G^{\frac{7}{2}}}{5c^5}\frac{\mu^2M^{\frac{5}{2}}}{a^5}\frac{1+\frac{7}{4}e^2}{(1-e^2)^2}\,, \tag{22}$$

Peters derived a system of two coupled ODEs for the secular time evolution of a and e. This system can be transformed into a decoupled ODE of the type $da/de = f(e)$, together with an ODE of the type $de/dt = g(e)/a^4$. The decoupled ODE $da/de = f(e)$ was explicitly solved by Peters with the result

$$a(e) = c_0\frac{e^{\frac{12}{19}}}{1-e^2}\left[1+\frac{121}{304}e^2\right]^{\frac{870}{2299}} \tag{23}$$

where c_0 is a constant of integration. The latter result shows that the eccentricity decreases as the semi-major axis decreases, and the orbital frequency

$$\Omega = \frac{2\pi}{P} = \sqrt{\frac{GM}{a^3}} \tag{24}$$

increases, under GW radiation reaction. [This decrease is roughly inversely proportional to the orbital frequency: $e \propto \Omega^{-\frac{19}{18}} \simeq \Omega^{-1}$.] In other words, radiation reaction

leads to a rather fast circularization of the binary orbit. As most coalescing compact binary systems will most likely enter the observable frequency band of ground-based interferometric GW detectors only after many years of secular evolution have led to a huge increase in orbital frequency, this brings the big simplification that observed binary systems can be expected to move on an orbit which can be well approximated by a secularly-shrinking *circular* orbit.

2.3 Early contributions to the theory of back holes (BH) (in brief)

Let us recall the discovery of BH solutions by Schwarzschild (1916) [11] and Kerr (1963) [12], and the pioneering work of Oppenheimer and Snyder (1939) [13], which introduced the vision of the dynamical formation of a BH during the collapse of a neutron star exceeding its maximum possible mass. In addition, especially important for the theoretical understanding of the post-merger, " ringdown" signal of coalescing BBH, one should mention the important discovery of [14] that the scattering of a featureless incoming Gaussian wavepacket on a BH generates, as outgoing wave, a wavepacket which features new oscillations, carrying information about the BH on which it scattered. This result initiated the vision of BHs as dynamical objects per se, instead of mere extreme potential wells, having a strange spacetime structure. It was later understood that the new oscillations imprinted on the outgoing wavepacket could be interpreted as "vibrations of the black hole" [15]. It was also found at the time that the fall of a particle in a BH would excite these "ringing modes" of the BH [16]. [The latter work belonged to the many investigations, done in the 1970's, of the possible GW signals emitted by test particles moving in BH backgrounds. These investigations made use of the Regge-Wheeler-Zerilli, and Teukolsky, formalisms for perturbed BH geometries.] The theory of these BH "Quasi-Normal Modes" (QNM) was later well developed, and is an important part of the GW signal emitted by a coalescing BBH. [They constitute the final, exponentially damped, part of the GW signal, called *"ringdown"*.]

3 Later history of accurate computations of the motion and radiation of binary systems

We have summarized above the early history of the description of the motion and GW emission of compact binaries (and notably binary black hole systems). This led to the *lowest-order* (LO) description of the secular inspiral, ending in a violent coalescence, of compact binaries. When plans for the construction of ultra-sensitive interferometric detectors of GWs started to materialize, it was, however, realized (see, e.g., [17]) that much more accurate descriptions of both the motion and the GW emission of binary systems were needed. Indeed, astrophysical estimates of the spacetime density of binary coalescences indicated that the signals to be expected would always be much smaller than the broadband noise of the detectors. Such a situation is far from new in physics and technology. In particular, the development of radar systems during the second world war led to many studies of the extraction of signals from noisy data stream. In the case where the signal to be extracted has a known shape, say $h^{\rm signal}(t;p_i)$ (depending, however, on the values of several a priori unkown parameters p_i), and when the background noise stream $n(t)$ is Gaussian and stationary, there is an optimal way of *filtering* the signal out of the observed noisy

output $h^{\rm obs}(t)$ of the detector, say

$$h^{\rm obs}(t) = n(t) + h^{\rm signal}(t; p_i) \tag{25}$$

This optimal filtering (called "Wiener filter") consists in computing a certain weigthed convolution between the detected noisy data stream $h^{\rm obs}(t)$ and a nearly continuous bank of *templates*, i.e. copies of the expected parameter-dependent signals $h^{\rm signal}(t; p_i)$. [Among the list of parameters p_i, there is always one, say $p_0 = t_0$, which describes the a priori unknown time of arrival of the signal.] In the time-domain the latter weighted convolution involves a kernel $K(t - t')$, which is the convolution-inverse of the noise correlation function $S_n(t - t') \equiv \overline{n(t)n(t')}$. In the frequency-domain, the convolution-inverse is simply the usual (algebraic) inverse, so that the optimal filter consists in computing the following weigthed *overlap*

$$\langle h^{\rm obs}(t), h^{\rm template}(t; p_i)\rangle = \int_{-\infty}^{+\infty} df \frac{e^{2\pi i f t_0}}{\tilde{S}_n(f)} \tilde{h}^{\rm obs} * (f)\, \tilde{h}^{\rm template}(f; p'_i) \tag{26}$$

Here, the tilde symbol denotes the Fourier transform, while p'_i denotes the list of parameters, excluding the time-delay one, which is parametrized by t_0 in the exponential factor $e^{2\pi i f t_0}$. [See the contribution of Eric Chassande-Mottin for details of the optimal filtering method, and of its application to data analysis.]

The overlap $\langle h^{\rm obs}(t), h^{\rm template}(t; p_i)\rangle$ is the sum of a random, zero-average noise-related term $\langle n(t), h^{\rm template}(t; p_i)\rangle$, and of a non-fluctuating, signal-related term $\langle h^{\rm signal}\ (t), h^{\rm template}(t; p_i)\rangle$. The crucial point is that the latter signal-related contribution will reach the maximum amplitude it can achieve (i.e. the maximum possible signal-to-noise-ratio) only if the templates $h^{\rm template}(t; p_i)$, used as filters, are very accurate representations (for some value of the parameters) of the expected real signals $h^{\rm signal}(t)$. Roughly speaking, this means that the template (of the type of Fig. 3) should (at least when the frequency of the GW signal is within the frequency range where the detector is reasonably sensitive, say between 30 Hz and 1000 Hz) only dephase from the real signal by a small fraction of a cycle. This requirement turned out to necessitate the development of new, sophisticated theoretical calculations of the motion and radiation of compact binaries, namely:

1. Development of analytical methods able to tackle the motion of strongly self-gravitating bodies, and notably of black holes;

2. Accurate analytical calculations of the motion of binary systems, going much beyond the LO (Newtonian) appproximation;

3. Accurate analytical calculations of the GW emission of binary systems, going much beyond the LO (quadrupole) appproximation;

4. Development of resummation methods, able to go beyond the limit of validity of the usual, PN approximation method, and thereby to describe the complete GW coalescence signal;

5. Development of *numerical* schemes able to tackle the inspiral and coalescence of black holes and neutron stars.

The following sections will briefly cover these developments.

4 Analytical developments in the general relativistic two-body problem

The two-body problem in General Relativity (GR), and notably the problem of the motion of compact bodies, has been the focus of many theoretical works, from the 1970's up until now. Indeed, the discovery in the 1970's of binary systems comprising strongly self-gravitating bodies (black holes or neutron stars) has obliged theorists to develop improved approaches to the two-body problem. These improved approaches are not limited (as the traditional PN method) to the case of weakly self-gravitating bodies and can be viewed as modern versions of the Einstein-Infeld-Hoffmann classic work [3].

In addition to the need of considering strongly self-gravitating bodies, the discovery of binary pulsars in the mid 1970's (starting with the Hulse-Taylor pulsar PSR $1913+16$) obliged theorists to go beyond the 1PN ($O(v^2/c^2)$) relativistic effects in the equations of motion (which was the level reached, notably, by Einstein, Infeld and Hoffmann [3]). More precisely, it was necessary to go to the 2.5PN approximation level, i.e. to include terms $O(v^5/c^5)$ beyond Newton in the equations of motion. This is, indeed, the level at which radiation reaction effects, linked to the finite velocity of propagation of the gravitational interaction between the two bodies, start entering the equations of motion. This was achieved in the 1980's by several groups [18, 19, 20, 21, 22]. [Let us note that important progress in obtaining the N-body metric and equations of motion at the 2PN level had been achieved by the Japanese school in the 1970's [23, 24, 25].] The main result of Refs. [18, 19, 20, 21, 22] was to show that the combination of the finite velocity of propagation of the gravitational interaction between the two bodies with the specific nonlinear properties of General Relativity implied a decay of the orbital period of a binary system given by the expression

$$\frac{dP}{dt} = -\frac{192\pi}{5c^5}\left(\frac{2\pi G}{P}\right)^{\frac{5}{3}} \mu M^{\frac{2}{3}} \frac{1+\frac{73}{24}e^2+\frac{37}{96}e^4}{(1-e^2)^{\frac{7}{2}}}\,. \tag{27}$$

The presence of a factor $1/c^5$ on the rhs corresponds to the fact that the effect (27) is linked to the 2.5PN, i.e. $O[(v/c)^5]$, contributions to the equations of motion of a binary system. The expression (27) can also be *heuristically* derived by requiring the balance (18) between the Newtonian energy of the binary system (20) and the LO GW energy flux (21). However, the works [18, 19, 20, 21, 22] were the first to derive the period decay (27) from Einstein's equations by means of a complete dynamical computation (taking into account, for the first time, all intermediate effects at 1PN and 2PN levels) based on the specific nonlinear properties of General Relativity together with the (assumed) propagation of gravity via a retarded Green's function. This result thereby showed that (contrary to what is often stated) the observed orbital period decay of binary pulsars is a *direct proof of the reality of gravitational radiation* (in the precise sense of the propagation at the velocity of light of the gravitational interaction between the two bodies). The often voiced contrary statement that the agreement between expression (27) and binary pulsar data is only an *indirect* proof of the existence of gravitational radiation is due to the use of the indirect reasoning that requires the energy balance (18). This indirect reasoning (which was the one used by Landau-Lifshitz, Dyson and Peters) heuristically relates a wave-zone energy loss to a near-zone binding-energy decrease, while the dynamical proof of (27) only involves dynamical quantities, and GW propagation effects, in the

near zone.

Motivation for pushing the accuracy of the equations of motion beyond the 2.5PN level came from the prospect of detecting the gravitational wave signal emitted by inspiralling and coalescing binary systems, notably binary neutron star (BNS) and binary black hole (BBH) systems. The 3PN-level equations of motion (including terms $O(v^6/c^6)$ beyond Newton) were derived in the late 1990's and early 2000's [26, 27, 28, 29, 30] (they have been rederived in [31]). The next-to-leading order radiation-reaction terms entering at the 3.5PN level ($O(v^7/c^7)$ beyond Newton) have been derived by several authors, starting with Ref. [32]. Recently, the (conservative) 4PN-level dynamics (including terms $O(v^8/c^8)$ beyond Newton) has been tackled in [33, 34, 35, 36, 37, 38] and completed in Refs. [39, 40] (the correctness of the latter 4PN dynamics has been confirmed in [41]).

Let us briefly contrast the new approaches to the problem of motion that have been developed after the 1970's to the older ones.

The traditional approach (started by Einstein, Droste, de Sitter, Eddington,...; see [42] for a review and references) to the problem of motion of N separate bodies in GR consists of solving, by successive approximations, Einstein's field equations (we use the signature $-+++$)

$$R_{\mu\nu} - \frac{1}{2}\, R\, g_{\mu\nu} = \frac{8\pi\, G}{c^4}\, T_{\mu\nu}\,, \tag{28}$$

together with their consequence

$$\nabla_\nu\, T^{\mu\nu} = 0\,. \tag{29}$$

To do so, one assumes some specific matter model, say a perfect fluid,

$$T^{\mu\nu} = (\varepsilon + p)\, u^\mu\, u^\nu + p\, g^{\mu\nu}\,. \tag{30}$$

One expands (say in powers of Newton's constant) the metric,

$$g_{\mu\nu}(x^\lambda) = \eta_{\mu\nu} + h^{(1)}_{\mu\nu} + h^{(2)}_{\mu\nu} + \dots\,, \tag{31}$$

and use the simplifications brought by the 'Post-Newtonian' approximation ($\partial_0\, h_{\mu\nu} = c^{-1}\, \partial_t\, h_{\mu\nu} \ll \partial_i\, h_{\mu\nu}$; $v/c \ll 1$, $p \ll \varepsilon$). Then one integrates the local material equation of motion (36) over the volume of each separate body, labelled say by $a = 1, 2, \dots, N$. In so doing, one must define some 'center of mass' z^i_a of body a, as well as some (approximately conserved) 'mass' m_a of body a, together with some corresponding 'spin vector' S^i_a and, possibly, higher multipole moments.

An important feature of this traditional method is to use a *unique coordinate chart* x^μ to describe the full N-body system. For instance, the center of mass, shape and spin of each body a are all described within this common coordinate system x^μ. This use of a single chart has several inconvenient aspects, even in the case of weakly self-gravitating bodies (as in the solar system case). Indeed, it means for instance that a body which is, say, spherically symmetric in its own 'rest frame' X^α will appear as deformed into some kind of ellipsoid in the common coordinate chart x^μ. Moreover, it is not clear how to construct 'good definitions' of the center of mass, spin vector, and higher multipole moments of body a, when described in the common coordinate chart x^μ. In addition, as we are possibly interested in the motion of strongly self-gravitating bodies, it is not a priori justified to use a simple

expansion of the type (31) because $h^{(1)}_{\mu\nu} \sim \sum_a Gm_a/(c^2\,|\boldsymbol{x}-\boldsymbol{z}_a|)$ will not be uniformly small in the common coordinate system x^μ. It will be small if one stays far away from each object a, but, it will become of order unity on the surface of a compact body.

These two shortcomings of the traditional 'one-chart' approach to the relativistic problem of motion can be cured by using a '*multi-chart' approach*. The multi-chart approach describes the motion of N (possibly, but not necessarily, compact) bodies by using $N+1$ separate coordinate systems: (i) one *global* coordinate chart x^μ ($\mu = 0,1,2,3$) used to describe the spacetime outside N 'tubes', each containing one body, and (ii) N *local* coordinate charts X^α_a ($\alpha = 0,1,2,3$; $a = 1,2,\ldots,N$) used to describe the spacetime in and around each body a. The multi-chart approach was first used to discuss the motion of black holes and other compact objects [43, 44, 45, 46, 47, 48, 49, 50, 51]. Then it was also found to be very convenient for describing, with the high-accuracy required for dealing with modern technologies such as VLBI, systems of N weakly self-gravitating bodies, such as the solar system [52, 53].

The essential idea of the multi-chart approach is to combine the information contained in *several expansions*. One uses both a global expansion of the type (31) and several local expansions of the type

$$G_{\alpha\beta}(X^\gamma_a) = G^{(0)}_{\alpha\beta}(X^\gamma_a; m_a) + H^{(1)}_{\alpha\beta}(X^\gamma_a; m_a, m_b) + \cdots\,, \tag{32}$$

where $G^{(0)}_{\alpha\beta}(X; m_a)$ denotes the (possibly strong-field) metric generated by an isolated body of mass m_a (possibly with the additional effect of spin).

The separate expansions (31) and (32) are then 'matched' in some overlapping domain of common validity of the type $Gm_a/c^2 \lesssim R_a \ll |\boldsymbol{x}-\boldsymbol{z}_a| \ll d \sim |\boldsymbol{x}_a - \boldsymbol{x}_b|$ (with $b \neq a$), where one can relate the different coordinate systems by expansions of the form

$$x^\mu = z^\mu_a(T_a) + e^\mu_i(T_a)\,X^i_a + \frac{1}{2}\,f^\mu_{ij}(T_a)\,X^i_a\,X^j_a + \cdots \tag{33}$$

The multi-chart approach becomes simplified if one considers *compact* bodies (of radius R_a comparable to $2\,Gm_a/c^2$). In this case, it was shown [49], by considering how the 'internal expansion' (32) propagates into the 'external' one (31) via the matching (33), that, *in General Relativity*, the internal structure of each compact body was *effaced* to a very high degree, when seen in the external expansion (31). For instance, for non spinning bodies, the internal structure of each body (notably the way it responds to an external tidal excitation) shows up in the external problem of motion only at the *fifth post-Newtonian* (5PN) approximation, i.e. in terms of order $(v/c)^{10}$ in the equations of motion.

This *'effacement of internal structure'* indicates that it should be possible to simplify the rigorous multi-chart approach by skeletonizing each compact body by means of some delta-function source. Mathematically, the use of distributional sources is delicate in a nonlinear theory such as GR. However, it was found that one can reproduce the results of the more rigorous matched-multi-chart approach by treating the divergent integrals generated by the use of delta-function sources by means of (complex) analytic continuation [49]. In particular, analytic continuation in the dimension of space d [54] is very efficient (especially at high PN orders).

Finally, the most efficient way to derive the general relativistic equations of motion of N compact bodies consists of solving the equations derived from the action (where $g \equiv -\det(g_{\mu\nu})$)

$$S = \int \frac{d^{d+1}\,x}{c}\,\sqrt{g}\,\frac{c^4}{16\pi\,G}\,R(g) - \sum_a m_a\,c\int\sqrt{-g_{\mu\nu}(z_a^\lambda)\,dz_a^\mu\,dz_a^\nu}\,, \tag{34}$$

formally using the standard weak-field expansion (31), but considering the space dimension d as an arbitrary complex number which is sent to its physical value $d=3$ only at the end of the calculation. This 'skeletonized' effective action approach to the motion of compact bodies has been extended to other theories of gravity [47, 48]. Finite-size corrections can be taken into account by adding nonminimal worldline couplings to the effective action (34) [55, 56].

5 PN-expanded results on the conservative dynamics of binary systems

It is convenient to decompose the dynamics of a binary system in two parts: (i) a conservative part (which is time-inversion-symmetric); and (ii) a dissipative part (which is time-antisymmetric).

The conservative dynamics of an isolated, gravitationally interacting two-body system is formally obtained by eliminating the gravitational field $g_{\mu\nu}$, conveying the time-symmetric (half-retarded-half-advanced) gravitational interaction, in the total (gauge-fixed) action $S_{\rm tot}[x_a^\mu;g_{\mu\nu}]$ describing the particles-plus-field system [57, 58, 59]. The so-obtained reduced (Fokker-type) action is then a functional $S[x_1^\mu,x_2^\nu]$ of the two worldlines. There are several ways of computing the latter reduced action. These several ways differ in: (1) the choice of coordinate gauge; (2) the encoding of the gravitational degrees of freedom; and (3) the technical way of computing the reduced action. Three prominent approaches to computing the reduced action are: (i) harmonic-gauge approach (as was used in the early 2.5PN work of [18, 19]); (ii) Arnowitt-Deser-Misner approach (as in Ref. [26]); and (iii) Effective Field Theory approach (as in Ref. [56]).

To give an idea of the structure of the reduced action $S[x_1^\mu,x_2^\nu]$, let us indicate how it looks when computed in harmonic gauge.

When working in the harmonic gauge, the Fokker action can be written as an infinite series $S_{\rm free}+S_{12}+\ldots$, where $S_{\rm free}=-\int m_1\,{\rm d}s_1-\int m_2\,{\rm d}s_2$ (with ${\rm d}s_a=\sqrt{-\eta_{\mu\nu}\,{\rm d}x_a^\mu\,{\rm d}x_a^\nu}$) is the free action, S_{12} the one-graviton-exchange interaction [60]

$$S_{12}[x_1,x_2] = 2G\iint {\rm d}s_1{\rm d}s_2\,t_1^{\mu\nu}(s_1)\;\mathcal{G}_{\mu\nu,\alpha\beta}(x_1(s_1)-x_2(s_2))\,t_2^{\alpha\beta}(s_2)\,, \tag{35}$$

with linear source terms $t_a^{\mu\nu}(s_a)=m_a({\rm d}x_a^\mu/{\rm d}s_a)({\rm d}x_a^\nu/{\rm d}s_a)$, gravitational propagator (in $D=4$ spacetime dimensions) $\mathcal{G}_{\mu\nu,\alpha\beta}=\left(\eta_{\mu\alpha}\,\eta_{\nu\beta}-\frac{1}{2}\,\eta_{\mu\nu}\,\eta_{\alpha\beta}\right)\mathcal{G}$, with $\mathcal{G}(x,x')\equiv -4\pi\,\Box^{-1}_{\rm sym}=\delta(\eta_{\mu\nu}(x^\mu-x'^\mu)(x^\nu-x'^\nu))$, and where the higher-order terms $+\ldots$ are given by more complicated Feynman-like integrals of the type (suppressing indices)

$$\begin{aligned} S_{112} \sim G^2 \iiiint {\rm d}s_1\,{\rm d}s_1'\,{\rm d}s_2\,{\rm d}^4x\,t_1(s_1)\,t_1(s_1')\,t_2(s_2) \\ \times\;\partial\partial\,\mathcal{G}(x_1-x)\,\mathcal{G}(x_1'-x)\,\mathcal{G}(x-x_2)\,, \end{aligned} \tag{36}$$

where the concatenation of source terms, propagators and vertices (here at the intermediate field point x) is defined by the (gauge-fixed) Einstein-Hilbert action [61]. The explicit form of the Poincaré-invariant equations of motion at order G^2 have been obtained in Refs. [62, 63]. For the definition and computation of the PN-expanded version of the harmonic-gauge Fokker action see Refs. [56, 64, 65, 66, 38].

Previous works [25, 22, 67] have shown that computing the reduced gravitational action by means of the canonical formalism of Arnowitt, Deser and Misner (ADM) [68] had several useful features. There are less propagating degrees of freedom in this approach than in harmonic gauge. Essentially g_{00} and g_{0i} have been eliminated, to leave only the spatial metric g_{ij} and its canonically conjugated momentum π^{ij}.

The computation of the reduced two-body action (in spacetime dimension $D \equiv d+1$) within the ADM formalism goes through several steps [see, e.g., Ref. [39] for a recent summary of these steps]. The details of the PN calculations of the conservative dynamics, as well as the form of the final results, depend on the approach taken. To be concrete, let us quote the explicit form of the final, PN-expanded two-body Hamiltonian at the 4PN approximation, as recently obtained (within the ADM formalism) in [39] (using the local results of [37]). For simplicity, we quote the results for the center-of-mass-reduced dynamics (with rescaled Hamiltonian $\widehat{H} \equiv H/\mu$), expressed in terms of scaled variables: $\mathbf{r} = (\mathbf{x}_1 - \mathbf{x}_2)/GM$, $\mathbf{p} = \mathbf{p}_1/\mu = -\mathbf{p}_2/\mu$, where

$$M \equiv m_1 + m_2 \quad , \quad \mu = \frac{m_1 m_2}{m_1 + m_2} \quad , \quad \nu \equiv \frac{\mu}{M} \equiv \frac{m_1 m_2}{(m_1 + m_2)^2} \tag{37}$$

$$\widehat{H}_{\rm N}\left(\mathbf{r},\mathbf{p}\right) = \frac{\mathbf{p}^2}{2} - \frac{1}{r}, \tag{38}$$

$$\widehat{H}_{\rm 1PN}\left(\mathbf{r},\mathbf{p}\right) = \frac{1}{8}(3\nu-1)(\mathbf{p}^2)^2 - \frac{1}{2}\Big\{(3+\nu)\mathbf{p}^2 + \nu(\mathbf{n}\cdot\mathbf{p})^2\Big\}\frac{1}{r} + \frac{1}{2r^2}, \tag{39}$$

$$\begin{aligned}\widehat{H}_{\rm 2PN}(\mathbf{r},\mathbf{p}) = {}& \frac{1}{16}(1-5\nu+5\nu^2)(\mathbf{p}^2)^3 \\ & + \frac{1}{8}\Big\{(5-20\nu-3\nu^2)(\mathbf{p}^2)^2 - 2\nu^2(\mathbf{n}\cdot\mathbf{p})^2\mathbf{p}^2 - 3\nu^2(\mathbf{n}\cdot\mathbf{p})^4\Big\}\frac{1}{r} \\ & + \frac{1}{2}\Big\{(5+8\nu)\mathbf{p}^2 + 3\nu(\mathbf{n}\cdot\mathbf{p})^2\Big\}\frac{1}{r^2} - \frac{1}{4}(1+3\nu)\frac{1}{r^3},\end{aligned} \tag{40}$$

$$\begin{aligned}\widehat{H}_{\rm 3PN}(\mathbf{r},\mathbf{p}) = {}& \frac{1}{128}(-5+35\nu-70\nu^2+35\nu^3)(\mathbf{p}^2)^4 \\ & + \frac{1}{16}\Big\{(-7+42\nu-53\nu^2-5\nu^3)(\mathbf{p}^2)^3 + (2-3\nu)\nu^2(\mathbf{n}\cdot\mathbf{p})^2(\mathbf{p}^2)^2 \\ & + 3(1-\nu)\nu^2(\mathbf{n}\cdot\mathbf{p})^4\mathbf{p}^2 - 5\nu^3(\mathbf{n}\cdot\mathbf{p})^6\Big\}\frac{1}{r}[2ex]\end{aligned}$$

$$
\begin{aligned}
&+\left\{\frac{1}{16}(-27+136\nu+109\nu^2)(\mathbf{p}^2)^2\right.\\
&\left.+\frac{1}{16}(17+30\nu)\nu(\mathbf{n}\cdot\mathbf{p})^2\mathbf{p}^2+\frac{1}{12}(5+43\nu)\nu(\mathbf{n}\cdot\mathbf{p})^4\right\}\frac{1}{r^2}\\
&+\left\{\Big(-\frac{25}{8}+\left(\frac{\pi^2}{64}-\frac{335}{48}\right)\nu-\frac{23\nu^2}{8}\Big)\mathbf{p}^2\right.\\
&+\left(-\frac{85}{16}-\frac{3\pi^2}{64}-\frac{7\nu}{4}\right)\nu(\mathbf{n}\cdot\mathbf{p})^2\frac{1}{r^3}\\
&\left.+\left\{\frac{1}{8}+\Big(\frac{109}{12}-\frac{21}{32}\pi^2\Big)\nu\right\}\frac{1}{r^4}.\right. \qquad (41)
\end{aligned}
$$

$$
\begin{aligned}
\widehat{H}_{\rm 4PN}(\mathbf{r},\mathbf{p}) &= \left(\frac{7}{256}-\frac{63}{256}\nu+\frac{189}{256}\nu^2-\frac{105}{128}\nu^3+\frac{63}{256}\nu^4\right)(\mathbf{p}^2)^5\\
&+\left\{\frac{45}{128}(\mathbf{p}^2)^4-\frac{45}{16}(\mathbf{p}^2)^4\,\nu+\left(\frac{423}{64}(\mathbf{p}^2)^4-\frac{3}{32}(\mathbf{n}\cdot\mathbf{p})^2(\mathbf{p}^2)^3-\frac{9}{64}(\mathbf{n}\cdot\mathbf{p})^4(\mathbf{p}^2)^2\right)\nu^2\right.\\
&+\left(-\frac{1013}{256}(\mathbf{p}^2)^4+\frac{23}{64}(\mathbf{n}\cdot\mathbf{p})^2(\mathbf{p}^2)^3+\frac{69}{128}(\mathbf{n}\cdot\mathbf{p})^4(\mathbf{p}^2)^2-\frac{5}{64}(\mathbf{n}\cdot\mathbf{p})^6\mathbf{p}^2+\frac{35}{256}(\mathbf{n}\cdot\mathbf{p})^8\right)\nu^3\\
&\left.+\left(-\frac{35}{128}(\mathbf{p}^2)^4-\frac{5}{32}(\mathbf{n}\cdot\mathbf{p})^2(\mathbf{p}^2)^3-\frac{9}{64}(\mathbf{n}\cdot\mathbf{p})^4(\mathbf{p}^2)^2-\frac{5}{32}(\mathbf{n}\cdot\mathbf{p})^6\mathbf{p}^2-\frac{35}{128}(\mathbf{n}\cdot\mathbf{p})^8\right)\nu^4\right\}\frac{1}{r}\\
&+\left\{\frac{13}{8}(\mathbf{p}^2)^3+\left(-\frac{791}{64}(\mathbf{p}^2)^3+\frac{49}{16}(\mathbf{n}\cdot\mathbf{p})^2(\mathbf{p}^2)^2-\frac{889}{192}(\mathbf{n}\cdot\mathbf{p})^4\mathbf{p}^2+\frac{369}{160}(\mathbf{n}\cdot\mathbf{p})^6\right)\nu\right.\\
&+\left(\frac{4857}{256}(\mathbf{p}^2)^3-\frac{545}{64}(\mathbf{n}\cdot\mathbf{p})^2(\mathbf{p}^2)^2+\frac{9475}{768}(\mathbf{n}\cdot\mathbf{p})^4\mathbf{p}^2-\frac{1151}{128}(\mathbf{n}\cdot\mathbf{p})^6\right)\nu^2\\
&\left.+\left(\frac{2335}{256}(\mathbf{p}^2)^3+\frac{1135}{256}(\mathbf{n}\cdot\mathbf{p})^2(\mathbf{p}^2)^2-\frac{1649}{768}(\mathbf{n}\cdot\mathbf{p})^4\mathbf{p}^2+\frac{10353}{1280}(\mathbf{n}\cdot\mathbf{p})^6\right)\nu^3\right\}\frac{1}{r^2}\\
&+\left\{\frac{105}{32}(\mathbf{p}^2)^2+\left(\left(\frac{2749\pi^2}{8192}-\frac{589189}{19200}\right)(\mathbf{p}^2)^2+\left(\frac{63347}{1600}-\frac{1059\pi^2}{1024}\right)(\mathbf{n}\cdot\mathbf{p})^2\mathbf{p}^2\right.\right.\\
&\quad\left.+\left(\frac{375\pi^2}{8192}-\frac{23533}{1280}\right)(\mathbf{n}\cdot\mathbf{p})^4\right)\nu\\
&\quad+\left(\left(\frac{18491\pi^2}{16384}-\frac{1189789}{28800}\right)(\mathbf{p}^2)^2+\left(-\frac{127}{3}-\frac{4035\pi^2}{2048}\right)(\mathbf{n}\cdot\mathbf{p})^2\mathbf{p}^2\right.\\
&\quad\left.\left.+\left(\frac{57563}{1920}-\frac{38655\pi^2}{16384}\right)(\mathbf{n}\cdot\mathbf{p})^4\right)\nu^2
\end{aligned}
$$

$$+\left(-\frac{553}{128}(\mathbf{p}^2)^2-\frac{225}{64}(\mathbf{n}\cdot\mathbf{p})^2\mathbf{p}^2-\frac{381}{128}(\mathbf{n}\cdot\mathbf{p})^4\right)\nu^3\Bigg\}\frac{1}{r^3}$$

$$+\left\{\frac{105}{32}\mathbf{p}^2+\left(\left(\frac{185761}{19200}-\frac{21837\pi^2}{8192}\right)\mathbf{p}^2+\left(\frac{3401779}{57600}-\frac{28691\pi^2}{24576}\right)(\mathbf{n}\cdot\mathbf{p})^2\right)\nu\right.$$

$$\left.+\left(\left(\frac{672811}{19200}-\frac{158177\pi^2}{49152}\right)\mathbf{p}^2+\left(\frac{110099\pi^2}{49152}-\frac{21827}{3840}\right)(\mathbf{n}\cdot\mathbf{p})^2\right)\nu^2\right\}\frac{1}{r^4}$$

$$+\left\{-\frac{1}{16}+\left(\frac{6237\pi^2}{1024}-\frac{169199}{2400}\right)\nu+\left(\frac{7403\pi^2}{3072}-\frac{1256}{45}\right)\nu^2\right\}\frac{1}{r^5}$$

$$-\frac{1}{5}\frac{G^2M}{\mu\,c^8}\,I^{(3)}_{ij}(t)\times\,\mathrm{Pf}_{2r_{12}/c}\int_{-\infty}^{+\infty}\frac{\mathrm{d}v}{|v|}\,I^{(3)}_{ij}(t+v) \tag{42}$$

The last contribution to the 4PN Hamiltonian, namely

$$H^{\mathrm{non\,loc}}_{\mathrm{4PN}}(t)=-\frac{1}{5}\frac{G^2M}{c^8}\,I^{(3)}_{ij}(t)\mathrm{Pf}_{2r_{12}/c}\int_{-\infty}^{+\infty}\frac{\mathrm{d}v}{|v|}\,I^{(3)}_{ij}(t+v)\,,$$

(where the symbol Pf_s denotes a Hadamard partie finie, with scale s) is *nonlocal in time*. The appearance of such a time-nonlocality in the dynamics of gravitationally interacting systems was first pointed out in Ref. [69].

Ref. [40] (see also [41]) showed how to "reduce" the above 4PN nonlocal dynamics to an ordinary time-local Hamiltonian dynamics by means of a procedure involving both a generalization of the usual higher-derivative-reduction method [70, 71, 72], and an action-angle (Delaunay) transformation method.

6 Accurate theory of the gravitational-wave emission of binary systems

The conservative dynamics of binary systems must be completed by a correspondingly accurate description of the GW emission, and of its back effect on the motion (radiation damping).

The original work of Einstein, and Landau-Lifshitz, on the LO GW emission of gravitationally interacting systems has been extended by many authors. One line of research followed Landau and Lifshitz in trying to directly solve Einstein's equations in harmonic coordinates, written in the form

$$\Box\,\mathfrak{h}^{\mu\nu}=\frac{16\pi G}{c^4}\tau^{\mu\nu}(\mathfrak{h}). \tag{43}$$

Here, $\eta^{\mu\nu}+\mathfrak{h}^{\mu\nu}\equiv\mathfrak{g}^{\mu\nu}\equiv\sqrt{g}g^{\mu\nu}$ denotes the "gothic" metric (which satisfies $0=\partial_\nu\mathfrak{g}^{\mu\nu}=\partial_\nu\mathfrak{h}^{\mu\nu}$ in harmonic coordinates), while $\Box\equiv\eta^{\mu\nu}\partial_\mu\partial_\nu$ denotes the flat d'Alembertian, and

$$\tau^{\mu\nu}=|g|T^{\mu\nu}+\frac{c^4}{16\pi G}\Lambda^{\mu\nu}(\mathfrak{h}) \tag{44}$$

denotes the "total effective stress-energy tensor", i.e. the sum of the (weight-one) stress-energy tensor of the matter, and of the (Landau-Lifshitz) "gravitational stress-energy tensor".

One can then try to solve the above harmonically-relaxed Einstein equations by successive iteration, i.e. by writing

$$\mathfrak{h}^{\mu\nu} = \frac{16\pi G}{c^4} \Box_R^{-1} \tau^{\mu\nu}(\mathfrak{h}), \tag{45}$$

where $\Box_R^{-1}$ is a retarded potential kernel, and by successively replacing $\mathfrak{h}$ on the rhs by a known, lower-order approximation of the $\mathfrak{h}$ entering the lhs.

This direct integration of the harmonically-relaxed Einstein equations (pioneered by Landau and Lifshitz) has been particularly pursued by Epstein, Wagoner and Will [73, 74, 75]. Though this method was pushed to the next-to-next-to-leading-order (NNLO) beyond the LO quadrupole formula [75], it seems less powerful than the method to be described next.

The most powerful, currently available analytical GW generation formalism is the *Multipolar Post-Minkowskian* (MPM) formalism. This formalism was introduced in [76], and developed in many later papers by Blanchet, Damour, Iyer and others. Among the key papers let us cite: [77, 78, 79, 80, 81, 82]. In particular, the latter paper was the first one to obtain the 3PN-accurate quadrupole moment needed to obtain the 3.5PN-level GW flux from a circular binary. This formalism makes use of a cocktail of rather sophisticated methods: mutipolar-expansion, crucial use of analytic continuation to iteratively solve Einstein's equations in the external zone, crucial use of dimensional regularization for treating the near-field of the two BHs, high-order PN expansion, use of matched-asymptotic-expansions.

Contrary to the "direct" method indicated above (based on iterating Eq. (45)), the MPM method looks for an iterative, post-Minkowskian (PM), solution, of the type

$$\mathfrak{h}^{\mu\nu} = G\mathfrak{h}_1^{\mu\nu} + G^2\mathfrak{h}_2^{\mu\nu} + G^3\mathfrak{h}_3^{\mu\nu} + \cdots \tag{46}$$

of the *vacuum* version of Eq. (43), i.e.

$$\Box\, \mathfrak{h}^{\mu\nu} = \Lambda^{\mu\nu}(\mathfrak{h}). \tag{47}$$

This leads to a sequence of (inhomogeneous) wave equations of the form

$$\Box\, \mathfrak{h}_1^{\mu\nu} = 0 \tag{48}$$

$$\Box\, \mathfrak{h}_2^{\mu\nu} = \Lambda_2^{\mu\nu}(\mathfrak{h}_1), \text{ etc.} \tag{49}$$

First, one parametrizes the most general (retarded) solution of Eq. (48) (submitted to the harmonicity constraint $\partial_\nu \mathfrak{h}_1^{\mu\nu} = 0$) in the form of a *multipolar expansion*[1]

$$\mathfrak{h}_1^{00} = -\frac{4}{c^2} \sum_{l\geq 0} \frac{(-)^\ell}{\ell!} \partial_L \left(\frac{I_L(t-r/c)}{r} \right) + \text{gauge} \tag{50}$$

$$\mathfrak{h}_1^{0i} = \frac{4}{c^3} \sum_{l\geq 1} \frac{(-)^\ell}{\ell!} \frac{\ell}{\ell+1} \epsilon_{iab} \partial_{aL-1} \left(\frac{J_{bL-1}(t-r/c)}{r} \right) + \cdots + \text{gauge}, \tag{51}$$

$$\mathfrak{h}_1^{ij} = \cdots + \text{gauge}, \tag{52}$$

[1]We use symmetric-trace-free Cartesian tensors of degree ℓ, such as I_L (ℓth mass tensor) and J_L (ℓth spin tensor) [where $L \equiv i_1 i_2 \cdots i_\ell$ denotes a multi-index of order ℓ] to parametrize the $2\ell+1$-dimensional irreducible representation of SO(3).

where the (harmonic) gauge terms involve other (gauge) multipole moments. Second, one solves the higher-order equations, such as Eq. (49) [using Eqs. (50), etc. to replace the rhs as a sum of multipolar-type *nonlinear* source terms $\propto \sum r^{-k} F_{kL}(t - r/c)n^L$, where $n^L = n^{i_1} n^{i_2} \cdots n^{i_\ell}$ is a multi-tensor product of the unit radial vector $n^i = x^i/r$] by means of an analytic-continuation-regularized retarded integral:

$$\Box\, \mathfrak{h}_2^{\mu\nu} = \mathrm{PF}_B \Box_R^{-1} \left[\frac{r^B}{r_0^B} \Lambda_2^{\mu\nu}(\mathfrak{h}_1) \right] + p_2^{\mu\nu} \tag{53}$$

Here $\Box_R^{-1}$ is a retarded integral, B is a complex number, PF_B denotes the partie finie (i.e. the coefficient of B^0) of the Laurent expansion [in (negative and positive) powers of B] of the rhs, and $p_2^{\mu\nu}$ denotes a specific additional homogeneous contribution, constructed so as to ensure the condition $\partial_\nu \mathfrak{h}_2^{\mu\nu} = 0$.

After having so-constructed the most general (modulo gauge) vacuum (retarded) solution outside the material source, one determines (in the form of a PN expansion) the values of the seed multipole moments I_L and J_L (together with the physically less significant additional gauge multipoles) as functionals of the stress-energy tensor of the material source by matching the exterior MPM solution $\mathfrak{h}^{\mu\nu}[I_L, J_L, \cdots] = G\mathfrak{h}_1^{\mu\nu}[I_L, J_L, \cdots] + G^2 \mathfrak{h}_2^{\mu\nu}[I_L, J_L, \cdots] + \cdots$ to the near-zone solution of the *inhomogeneous* Einstein equations constructed by the usual PN approximation method. The latter matching leads (at each given PN accuracy) to an explicit determination of the relation between the seed multipole moments, I_L, J_L, $\cdots$, and the stress-energy tensor of the material source. This matching was performed at the 1PN order, in an explicit way, in Refs.[77] and [83]. Later, Blanchet [79] [80] derived a useful general formula directly relating the seed multipole moments of (a certain version of) the MPM algorithm to the source. The result of Blanchet (which crucially uses various properties of the convergence factor $(r/r_0)^B$, together with analytic continuation, and partie finie, in B) consists in showing that (in a suitable gauge) the MPM multipole moments can simply be written as the multipole moments of linearized gravity [78], with the Landau-Lifshitz-type replacement

$$T^{\mu\nu}_{\mathrm{linearizedGR}} \to \left(\frac{r}{r_0} \right)^B \tau^{\mu\nu}(\mathfrak{h}). \tag{54}$$

The nonlinear iterations of the MPM formalism automatically include the *hereditary* effects of GWs in the wavezone (i.e. the so-called "tails"). These hereditary effects affect the functional structure of the "radiative multipole moments", $U_L(U)$ and $V_L(U)$ that parametrize the waveform observed far from a binary system. [Here $U = t - r/c - 2(G\mathrm{M}/c^3)\ln(r/r_0) + \cdots$, with M denoting ADM mass of the system, is a Bondi-type retarded time in the wavezone.] Indeed, the functional relation between the radiative multipole moments $U_L(U)$ and $V_L(U)$ and the source involve not only (like in the LO quadrupole formula) time-derivatives of the multipole moments of the system at the retarded time U, but also *integrals* involving the behavior of the multipole moments on retarded times *anterior* to the observer retarded time U. For instance, the radiative quadrupole moment at infinity has an expansion of the type [84]

$$U_{ij}(U) = I_{ij}^{(2)}(U) + \frac{2G\mathrm{M}}{c^3} \int_0^{+\infty} \mathrm{d}\tau \left[\ln\left(\frac{c\tau}{2r_0} \right) + \frac{11}{12} \right] I_{ij}^{(4)}(U - \tau) \tag{55}$$

$$+2\left(\frac{G\mathrm{M}}{c^3}\right)^2\int_0^{+\infty}\mathrm{d}\tau\left[\ln^2\left(\frac{c\tau}{2r_0}\right)+\frac{57}{70}\ln\left(\frac{c\tau}{2r_0}\right)+\frac{124627}{44100}\right]\mathrm{M}_{ij}^{(5)}(U-\tau)+\cdots\,.$$

Using the powerful MPM formalism, together with dimensional regularization for dealing with the strong self-gravity of compact objects (such as black holes), it was possible to compute the GW emission of binary systems up to a high PN order. In particular, both the individual radiative multipole moments, and the corresponding GW energy flux, were computed to high PN accuracy for binary systems moving on circular orbits (which is the most important situation for GW detections, in view of the result of Peters mentioned above). For instance, the 3.5PN-accurate GW energy flux emitted by a circular binary system of orbital frequency Ω, expressed in terms of the dimensionless frequency parameter

$$x\equiv\left(\frac{GM\Omega}{c^3}\right)^{\frac{2}{3}}\,, \tag{56}$$

reads (from Refs. [82], [84] and references therein)

$$\begin{aligned}F_{GW}^{E}(x)=\frac{32c^5}{5G}\nu^2x^5\Bigg\{&1+\left(-\frac{1247}{336}-\frac{35}{12}\nu\right)x+4\pi x^{3/2}\\&+\left(-\frac{44711}{9072}+\frac{9271}{504}\nu+\frac{65}{18}\nu^2\right)x^2+\left(-\frac{8191}{672}-\frac{583}{24}\nu\right)\pi x^{5/2}\\&+\left[\frac{6643739519}{69854400}+\frac{16}{3}\pi^2-\frac{1712}{105}\gamma_{\mathrm{E}}-\frac{856}{105}\ln(16\,x)\right.\\&\qquad\left.+\left(-\frac{134543}{7776}+\frac{41}{48}\pi^2\right)\nu-\frac{94403}{3024}\nu^2-\frac{775}{324}\nu^3\right]x^3\\&+\left(-\frac{16285}{504}+\frac{214745}{1728}\nu+\frac{193385}{3024}\nu^2\right)\pi x^{7/2}+\mathcal{O}\left(\frac{1}{c^8}\right)\Bigg\}\,.\end{aligned} \tag{57}$$

Here, the prefactor, $\frac{32c^5}{5G}\nu^2x^5$, is the LO result, obtained by using the Einstein-Landau-Lifshitz quadrupole formula, while the following bracket, $\big\{1+\big(-\frac{1247}{336}-\frac{35}{12}\nu\big)\,x+\cdots\big\}$, represents the fractional 3.5PN correction. For a review of more results concerning both the motion, and the GW radiation, of binary systems see Ref. [84].

7 The Effective One-Body Formalism

Around 1998, it was clearly realized that the sort of high-order PN-expanded analytical results on the motion and radiation of binary systems briefly summarized above would be insufficient (if used as they are) for allowing one to describe the last orbits, and the merger of binary black holes. Indeed, the issue is that the formal small expansion parameter $\epsilon=v/c$ [which can be defined as $v/c\equiv x^{\frac{1}{2}}\equiv(GM\Omega/c^3)^{\frac{1}{3}}$] becomes of order unity near the end of the inspiral, so that the various PN-expanded representations of both the dynamics, and the GW emission, of the type $c_0+c_1\,v/c+c_2\,v^2/c^2+c_3\,v^3/c^3+\cdots+c_n\,v^n/c^n$, become numerically useless before one can reach the merger. [For instance, the coefficient of the 3PN fractional correction ($\propto x^3=(v/c)^6$) in the 3.5PN GW flux (57) is numerically of order ~ 120 when

$v/c = x^{\frac{1}{2}} = \frac{1}{2}$ (corresponding to the merger of BBHs), so that the 3PN fractional correction to the LO quadrupole result is larger than 100 % at merger.]

In front of this situation, some authors [85] ascertained the "inability of current computational techniques to evolve a BBH through its last ~ 10 orbits of inspiral" and to compute the merger, and concluded to the necessity of describing the late inspiral and merger of BBHs by *numerical simulations*. By contrast, other authors [86] advocated the use of *resummation methods* for extending the domain of validity of the PN-acquired information to the late inspiral, and to the merger.

A resummation method consists in replacing a Taylor-like truncated expansion $c_0 + c_1\, v/c + c_2\, v^2/c^2 + c_3\, v^3/c^3 + \cdots + c_n\, v^n/c^n$ by some non-polynomial function of v/c, defined so as to incorporate some of the expected non-perturbative features of the exact result. In 1999-2000 a new approach, called the Effective One-Body (EOB) formalism, to the resummation of the conservative dynamics of binary systems was introduced [87, 88, 89]. It was initially introduced for non-spinning binary systems, and was soon extended to the case of spinning systems [90].

The basic ideas and techniques for resumming each aspect of the motion, and radiation, of binary systems are different and have different historical roots.

Concerning the first ingredient, *i.e.* the EOB Hamiltonian, it was inspired by an approach to electromagnetically interacting quantum two-body systems introduced by Brézin, Itzykson and Zinn-Justin [91].

The resummation of the second ingredient, *i.e.* the EOB radiation-reaction force $\mathcal{F}$, was initially inspired by the Padé resummation of the flux function introduced by Damour, Iyer and Sathyaprakash [86]. More recently, a new and more sophisticated resummation technique for the (waveform and the) radiation reaction force $\mathcal{F}$ has been introduced by Damour, Iyer and Nagar [92, 93]. It will be discussed in detail below.

As for the third ingredient, *i.e.* the EOB description of the waveform emitted by a coalescing black hole binary, it was inspired by the work of Davis, Ruffini and Tiomno [16] which discovered the transition between the plunge signal and a ringing tail when a particle falls into a black hole. Additional motivation for the EOB treatment of the transition from plunge to ring-down came from work on the, so-called, "close limit approximation" [94].

Let us sketch here the approach used in the EOB formalism to resum the *conservative dynamics* of non-spinning binary systems. This approach (which gives its name to the entire formalism) is a general relativistic generalization of the well-known Newtonian-dynamics fact that the relative dynamics of a two-body system, with masses m_1, m_2 and interaction energy $V(\mathbf{x}_1 - \mathbf{x}_2)$, is equivalent to the dynamics of a test-particle of mass $\mu = m_1 m_2/(m_1 + m_2)$ and position $\mathbf{x} = \mathbf{x}_1 - \mathbf{x}_2$ submitted to the *same* potential energy $V(\mathbf{x})$. In the case of a gravitational two-body interaction, i.e. when $V(\mathbf{x}_1 - \mathbf{x}_2) = -Gm_1m_2/|\mathbf{x}_1 - \mathbf{x}_2|$, the identity $m_1 m_2 \equiv \mu M$ (where $M \equiv m_1 + m_2$) means that the gravitational two-body Newtonian interaction is equivalent to the dynamics of a mass μ attracted by a central mass $GM = G(m_1 + m_2)$.

The EOB approach generalizes this fact by looking for an 'effective external spacetime geometry' $g^{\rm eff}_{\mu\nu}(x^\lambda; GM, \nu)$ such that the geodesic dynamics of a 'test particle' of mass μ within $g^{\rm eff}_{\mu\nu}(x^\lambda, GM, \nu)$ is *equivalent* (when expanded in powers of $1/c^2$) to the original, relative PN-expanded dynamics (described by the PN-expanded

Hamiltonian (41)).

Let us explain the idea, proposed in [87], for establishing a 'dictionary' between the real relative-motion dynamics, (41), and the dynamics of an 'effective' particle of mass μ moving in $g^{\rm eff}_{\mu\nu}(x^\lambda, GM, \nu)$. The idea consists in 'thinking quantum mechanically'[2]. Instead of thinking in terms of a classical Hamiltonian, $H(\boldsymbol{q},\boldsymbol{p})$, and of its classical bound orbits, we can think in terms of the quantized energy levels $E(n,\ell)$ of the quantum bound states of the Hamiltonian operator $H(\hat{\boldsymbol{q}},\hat{\boldsymbol{p}})$. These energy levels will depend on two (integer valued) quantum numbers n and ℓ. Here (for a spherically symmetric interaction, as appropriate to $H^{\rm relative}$), ℓ parametrizes the total orbital angular momentum ($\boldsymbol{L}^2 = \ell(\ell+1)\,\hbar^2$), while n represents the 'principal quantum number' $n = \ell + n_r + 1$, where n_r (the 'radial quantum number') denotes the number of nodes in the radial wave function. The third 'magnetic quantum number' m (with $-\ell \leq m \leq \ell$) does not enter the energy levels because of the spherical symmetry of the two-body interaction (in the center of mass frame). For instance, the non-relativistic Newton interaction (Eq. (38)) gives rise to the well-known result

$$E_0(n,\ell) = -\frac{1}{2}\,\mu\left(\frac{GM\mu}{n\,\hbar}\right)^2 , \tag{58}$$

which depends only on n (this is the famous Coulomb degeneracy). When considering the PN corrections to H_0 one gets a more complicated expression of the form

$$E^{\rm relative}_{\rm PN}(n,\ell) = -\frac{1}{2}\mu\frac{\alpha^2}{n^2}\Bigg[1 + \frac{\alpha^2}{c^2}\left(\frac{c_{11}}{n\ell} + \frac{c_{20}}{n^2}\right)$$

$$+\frac{\alpha^4}{c^4}\left(\frac{c_{13}}{n\ell^3} + \frac{c_{22}}{n^2\ell^2} + \frac{c_{31}}{n^3\ell} + \frac{c_{40}}{n^4}\right) + \frac{\alpha^6}{c^6}\left(\frac{c_{15}}{n\ell^5} + \ldots + \frac{c_{60}}{n^6} + \cdots\right)\Bigg], \tag{59}$$

where we have set $\alpha \equiv GM\mu/\hbar = G\,m_1\,m_2/\hbar$, and where we consider, for simplicity, the (quasi-classical) limit where n and ℓ are large numbers. The 2PN-accurate version of Eq. (59) had been derived by Damour and Schäfer [95] as early as 1988 while its 3PN-accurate version was derived by Damour, Jaranowski and Schäfer in 1999 [96]. The dimensionless coefficients c_{pq} are functions of the symmetric mass ratio $\nu \equiv \mu/M$, for instance $c_{40} = \frac{1}{8}(145 - 15\nu + \nu^2)$. In classical mechanics (*i.e.* for large n and ℓ), it is called the 'Delaunay Hamiltonian', *i.e.* the Hamiltonian expressed in terms of the *action variables*[3] $J = \ell\hbar = \frac{1}{2\pi}\oint p_\varphi\, d\varphi$, and $N = n\hbar = I_r + J$, with $I_r = \frac{1}{2\pi}\oint p_r\, dr$.

The (PN-expanded) energy levels (59) encode, in a *gauge-invariant* way, the relative dynamics of a 'real' binary. Let us now consider an auxiliary problem: the 'effective' dynamics of one body, of mass μ, following (modulo the Q term discussed below) a geodesic in some ν-dependent 'effective external' (spherically symmetric) metric[4]

$$g^{\rm eff}_{\mu\nu}\,dx^\mu\,dx^\nu = -A(R;\nu)\,c^2\,dT^2 + B(R;\nu)\,dR^2 + R^2(d\theta^2 + \sin^2\theta\,d\varphi^2)\,. \tag{60}$$

[2]This is related to an idea emphasized many times by John Archibald Wheeler: quantum mechanics can often help us in going to the essence of classical mechanics.

[3]We consider, for simplicity, 'equatorial' motions with $m = \ell$, *i.e.*, classically, $\theta = \frac{\pi}{2}$.

[4]It is convenient to write the 'effective metric' in Schwarzschild-like coordinates. Note that the effective radial coordinate R differs from the two-body ADM-coordinate relative distance $R^{\rm ADM} = |\boldsymbol{q}|$. The transformation between the two coordinate systems has been determined in Refs. [87, 97].

Here, the *a priori unknown* metric functions $A(R;\nu)$ and $B(R;\nu)$ will be constructed in the form of expansions in GM/c^2R:

$$A(R;\nu) = 1 + \widetilde{a}_1 \frac{GM}{c^2R} + \widetilde{a}_2 \left(\frac{GM}{c^2R}\right)^2 + \widetilde{a}_3 \left(\frac{GM}{c^2R}\right)^3 + \widetilde{a}_4 \left(\frac{GM}{c^2R}\right)^4 + \cdots ;$$
$$B(R;\nu) = 1 + \widetilde{b}_1 \frac{GM}{c^2R} + \widetilde{b}_2 \left(\frac{GM}{c^2R}\right)^2 + b_3 \left(\frac{GM}{c^2R}\right)^3 + \cdots , \tag{61}$$

where the dimensionless coefficients $\widetilde{a}_n, \widetilde{b}_n$ depend on ν. From the Newtonian limit, it is clear that we should set $\widetilde{a}_1 = -2$. In addition, as ν can be viewed as a deformation parameter away from the test-mass limit, we require that the effective metric (60) tend to the Schwarzschild metric (of mass M) as $\nu \to 0$, *i.e.* that

$$A(R;\nu=0) = 1 - 2GM/c^2R = B^{-1}(R;\nu=0)\,.$$

Let us now require that the dynamics of the "one body" μ within the effective metric $g^{\rm eff}_{\mu\nu}$ be described by an "effective" mass-shell condition of the form

$$g^{\mu\nu}_{\rm eff}\, p^{\rm eff}_\mu\, p^{\rm eff}_\nu + \mu^2\, c^2 + Q(p^{\rm eff}_\mu) = 0\,,$$

where $Q(p)$ is (at least) *quartic* in p. Then by solving (by separation of variables) the corresponding 'effective' Hamilton-Jacobi equation

$$g^{\mu\nu}_{\rm eff} \frac{\partial S_{\rm eff}}{\partial x^\mu} \frac{\partial S_{\rm eff}}{\partial x^\nu} + \mu^2 c^2 + Q\left(\frac{\partial S_{\rm eff}}{\partial x^\mu}\right) = 0\,,$$
$$S_{\rm eff} = -\mathcal{E}_{\rm eff}\, t + J_{\rm eff}\, \varphi + S_{\rm eff}(R)\,, \tag{62}$$

one can straightforwardly compute (in the quasi-classical, large quantum numbers limit) the effective Delaunay Hamiltonian $\mathcal{E}_{\rm eff}(N_{\rm eff}, J_{\rm eff})$, with $N_{\rm eff} = n_{\rm eff}\,\hbar$, $J_{\rm eff} = \ell_{\rm eff}\,\hbar$ (where $N_{\rm eff} = J_{\rm eff} + I^{\rm eff}_R$, with $I^{\rm eff}_R = \frac{1}{2\pi}\oint p^{\rm eff}_R\, dR$, $P^{\rm eff}_R = \partial S_{\rm eff}(R)/dR$). This yields a result of the form

$$\mathcal{E}_{\rm eff}(n_{\rm eff}, \ell_{\rm eff}) = \mu c^2 - \frac{1}{2}\,\mu\, \frac{\alpha^2}{n^2_{\rm eff}} \Bigg[1 + \frac{\alpha^2}{c^2}\left(\frac{c^{\rm eff}_{11}}{n_{\rm eff}\ell_{\rm eff}} + \frac{c^{\rm eff}_{20}}{n^2_{\rm eff}}\right)$$
$$+ \frac{\alpha^4}{c^4}\left(\frac{c^{\rm eff}_{13}}{n_{\rm eff}\ell^3_{\rm eff}} + \frac{c^{\rm eff}_{22}}{n^2_{\rm eff}\ell^2_{\rm eff}} + \frac{c^{\rm eff}_{31}}{n^3_{\rm eff}\ell_{\rm eff}} + \frac{c^{\rm eff}_{40}}{n^4_{\rm eff}}\right)$$
$$+ \frac{\alpha^6}{c^6}\left(\frac{c^{\rm eff}_{15}}{n_{\rm eff}\ell^5_{\rm eff}} + \ldots + \frac{c^{\rm eff}_{60}}{n^6_{\rm eff}}\right) + \cdots\Bigg], \tag{63}$$

where the dimensionless coefficients $c^{\rm eff}_{pq}$ are now functions of the unknown coefficients $\widetilde{a}_n, \widetilde{b}_n$ entering the looked for 'external' metric coefficients (61).

At this stage, one needs to define a 'dictionary' between the real (relative) two-body dynamics, summarized in Eq. (59), and the effective one-body one, summarized in Eq. (63). As, on both sides, quantum mechanics tells us that the action variables are quantized in integers ($N_{\rm real} = n\hbar$, $N_{\rm eff} = n_{\rm eff}\hbar$, etc.) it is most natural to identify $n = n_{\rm eff}$ and $\ell = \ell_{\rm eff}$. One then still needs a rule for relating the two different energies $E^{\rm relative}_{\rm real}$ and $\mathcal{E}_{\rm eff}$. Ref. [87] proposed to look for a general map between the real energy

levels and the effective ones (which, as seen when comparing (59) and (63), cannot be directly identified because they do not include the same rest-mass contribution[5]), namely

$$\frac{\mathcal{E}_{\rm eff}}{\mu c^2} - 1 = f\left(\frac{E^{\rm relative}_{\rm real}}{\mu c^2}\right) = \frac{E^{\rm relative}_{\rm real}}{\mu c^2}\left(1 + \alpha_1 \frac{E^{\rm relative}_{\rm real}}{\mu c^2} + \alpha_2 \left(\frac{E^{\rm relative}_{\rm real}}{\mu c^2}\right)^2 + \alpha_3 \left(\frac{E^{\rm relative}_{\rm real}}{\mu c^2}\right)^3 + \dots\right). \tag{64}$$

The 'correspondence' between the real and effective energy levels is illustrated in Fig. 4.

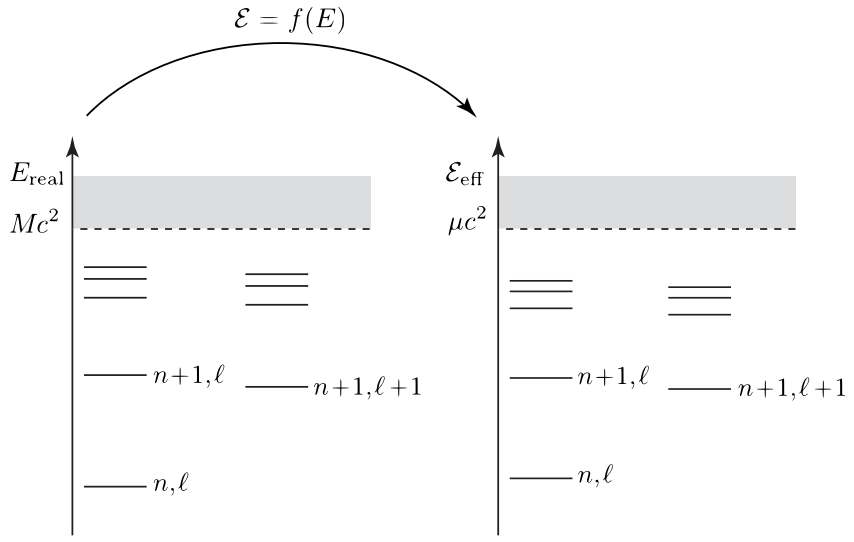

Figure 4: Sketch of the correspondence between the quantized energy levels of the real and effective conservative dynamics. n denotes the 'principal quantum number' ($n = n_r + \ell + 1$, with $n_r = 0, 1, \dots$ denoting the number of nodes in the radial function), while ℓ denotes the (relative) orbital angular momentum ($\boldsymbol{L}^2 = \ell(\ell+1)\,\hbar^2$). Though the EOB method is purely classical, it is conceptually useful to think in terms of the underlying (Bohr-Sommerfeld) quantization conditions of the action variables I_R and J to motivate the identification between n and ℓ in the two dynamics.

Finally, identifying $\mathcal{E}_{\rm eff}(n,\ell)/\mu c^2$ to $1 + f(E^{\rm relative}_{\rm real}(n,\ell)/\mu c^2)$ yields a system of equations for determining the unknown EOB coefficients $\widetilde{a}_n, \widetilde{b}_n, \alpha_n$, as well as the coefficients parametrizing a general quartic mass-shell deformation. [The need for introducing a quartic mass-shell deformation Q only arises at the 3PN level.]

Let us quote the result of solving this system of equations at the 3PN level (as obtained in Ref. [97]). The three EOB potentials A, D, Q describing the two-body dynamics are given (at the 3PN level) by very simple functions of the EOB "gravitational potential" $u \equiv \frac{GM}{c^2 R}$. With the short-hand notation

$$a_4 = \frac{94}{3} - \frac{41}{32}\,\pi^2 \simeq 18.6879027\ , \tag{65}$$

[5] Indeed $E^{\rm total}_{\rm real} = Mc^2 + E^{\rm relative}_{\rm real} = Mc^2 + \text{Newtonian terms} + 1\text{PN}/c^2 + \cdots$, while $\mathcal{E}_{\rm effective} = \mu c^2 + N + 1\text{PN}/c^2 + \cdots$.

for the 3PN-level coefficient entering the radial potential $A(R;\nu)$, one finds

$$A_{\rm 3PN}(R) = 1 - 2u + 2\,\nu\,u^3 + a_4\,\nu\,u^4\,, \tag{66}$$

$$D_{\rm 3PN}(R) \equiv (A(R)B(R))_{\rm 3PN} = 1 - 6\nu u^2 + 2(3\nu - 26)\nu u^3\ , \tag{67}$$

$$Q_{\rm 3PN}(\boldsymbol{q},\boldsymbol{p}) = \frac{1}{c^2}\,2(4-3\nu)\nu\ u^2\ \frac{p_r^4}{\mu^2}\,. \tag{68}$$

In addition, the map between the (real) center-of-mass energy of the binary system $E^{\rm relative}_{\rm real} = H^{\rm relative} = \mathcal{E}^{\rm tot}_{\rm relative} - Mc^2$ and the effective one $\mathcal{E}_{\rm eff}$ is found to have the very simple (but non trivial) form

$$\frac{\mathcal{E}_{\rm eff}}{\mu c^2} = 1 + \frac{E^{\rm relative}_{\rm real}}{\mu c^2}\left(1 + \frac{\nu}{2}\,\frac{E^{\rm relative}_{\rm real}}{\mu c^2}\right) = \frac{s - m_1^2\,c^4 - m_2^2\,c^4}{2\,m_1\,m_2\,c^4} \tag{69}$$

where $s = (\mathcal{E}^{\rm tot}_{\rm real})^2 \equiv (Mc^2 + E^{\rm relative}_{\rm real})^2$ is Mandelstam's invariant $s = -(p_1+p_2)^2$.

It is truly remarkable that the EOB formalism succeeds in *condensing* the complicated, original 3PN Hamiltonian, Eqs. (41), into the very simple potentials A, D and Q displayed above, together with the simple energy map Eq. (69). This simplicity of the EOB results is not only due to the reformulation of the PN-expanded Hamiltonian into an effective dynamics, but also follows from several remarkable cancellations taking place in the ν-dependence of the EOB $A(u;\nu)$ potential.

The large value of the a_4 coefficient happens to prevent the PN-expanded potential $A_{\rm 3PN}$ to be qualitatively similar (as ν increases up to $\frac{1}{4}$) to the Schwarzschild potential $A_{\rm Schwarz}(u) = 1 - 2u$ in exhibiting, notably, a simple zero ("horizon"). It was therefore suggested [97] to further resum[6] $A_{\rm 3PN}(R)$ by replacing it by a suitable Padé (P) approximant. The replacement of $A_{\rm 3PN}(R)$ by[7]

$$A^1_3(R) \equiv P^1_3[A_{\rm 3PN}(R)] = \frac{1 + n_1 u}{1 + d_1 u + d_2 u^2 + d_3 u^3} \tag{70}$$

ensures that the $\nu = \frac{1}{4}$ case is smoothly connected with the $\nu = 0$ limit.

The 4PN-level EOB Hamiltonian has been determined in [40].

8 EOB description of radiation reaction and of the emitted waveform during inspiral

In the previous Section we have described how the EOB method encodes the conservative part of the relative orbital dynamics into the dynamics of an 'effective' particle. Let us now briefly discuss how to complete the EOB dynamics by defining some *resummed* expressions describing radiation reaction effects, and the corresponding waveform emitted at infinity. One is interested in circularized binaries, which have lost their initial eccentricity under the influence of radiation reaction. For such systems, it is enough (in first approximation [**?**]) to include a radiation reaction force in

[6] The PN-expanded EOB building blocks $A_{\rm 3PN}(R), B_{\rm 3PN}(R), \ldots$ already represent a *resummation* of the PN dynamics in the sense that they have "condensed" the many terms of the original PN-expanded Hamiltonian within a very concise format. But one should not refrain to further resum the EOB building blocks themselves, if this is physically motivated.

[7] We recall that the coefficients n_1 and (d_1, d_2, d_3) of the $(1,3)$ Padé approximant $P^1_3[A_{\rm 3PN}(u)]$ are determined by the condition that the first four terms of the Taylor expansion of A^1_3 in powers of $u = GM/(c^2R)$ coincide with $A_{\rm 3PN}$.

the p_φ equation of motion only. More precisely, we are using phase space variables $r, p_r, \varphi, p_\varphi$ associated with polar coordinates (in the equatorial plane $\theta = \frac{\pi}{2}$). Actually it is convenient to replace the radial momentum p_r by the momentum conjugate to the 'tortoise' radial coordinate $R_* = \int dR (B/A)^{1/2}$, *i.e.* $P_{R_*} = (A/B)^{1/2} P_R$. The real EOB Hamiltonian is obtained by first solving Eq. (69) to get $H^{\rm total}_{\rm real} = \sqrt{s}$ in terms of $\mathcal{E}_{\rm eff}$, and then by solving the effective Hamilton-Jacobi equation to get $\mathcal{E}_{\rm eff}$ in terms of the effective phase space coordinates $\boldsymbol{q}_{\rm eff}$ and $\boldsymbol{p}_{\rm eff}$. The result is given by two nested square roots (we henceforth set $c = 1$):

$$\hat{H}_{\rm EOB}(r, p_{r_*}, \varphi) = \frac{H^{\rm real}_{\rm EOB}}{\mu} = \frac{1}{\nu} \sqrt{1 + 2\nu \left(\hat{H}_{\rm eff} - 1\right)}\,, \tag{71}$$

where (at the 3PN level)

$$\hat{H}_{\rm eff} = \sqrt{p^2_{r_*} + A(r) \left(1 + \frac{p^2_\varphi}{r^2} + z_3 \frac{p^4_{r_*}}{r^2}\right)}\,, \tag{72}$$

with $z_3 = 2\nu\,(4 - 3\nu)$. Here, we are using suitably rescaled dimensionless (effective) variables: $r = R/GM$, $p_{r_*} = P_{R_*}/\mu$, $p_\varphi = P_\varphi/\mu GM$, as well as a rescaled time $t = T/GM$. This leads to equations of motion for $(r, \varphi, p_{r_*}, p_\varphi)$ of the form

$$\frac{d\varphi}{dt} = \frac{\partial\, \hat{H}_{\rm EOB}}{\partial\, p_\varphi} \equiv \Omega\,, \tag{73}$$

$$\frac{dr}{dt} = \left(\frac{A}{B}\right)^{1/2} \frac{\partial\, \hat{H}_{\rm EOB}}{\partial\, p_{r_*}}\,, \tag{74}$$

$$\frac{dp_\varphi}{dt} = \hat{\mathcal{F}}_\varphi\,, \tag{75}$$

$$\frac{dp_{r_*}}{dt} = -\left(\frac{A}{B}\right)^{1/2} \frac{\partial\, \hat{H}_{\rm EOB}}{\partial\, r}\,. \tag{76}$$

The EOB resummation of the φ component of the radiation reaction, $\hat{\mathcal{F}}_\varphi$, i.e., which has been introduced on the r.h.s. of Eq. (75), will be discussed below.

8.1 The first prediction of the complete GW signal emitted by coalescing BBHs

The EOB formalism led to *the first (approximate) computation of the full coalescence waveform*, from inspiral to ringdown, going through the coalescence of the BBH. Indeed, the work of Buonanno and Damour [88], proposed to complete the EOB Hamiltonian of [87] (describing the conservative dynamics) by an additional radiation-damping force computed by using the "non-perturbative resummation technique" previously introduced in [86]. This proposal led to the first analytical description of the last orbits of a binary black hole (BBH) system, up to coalescence, and made several quantitative and qualitative predictions concerning the dynamics of the coalescence and the corresponding waveform: (i) a blurred transition from inspiral to "plunge" that is just a smooth continuation of the inspiral, and (ii) a sharp transition, around the merger of the BBH, between a continued inspiral and a ringdown signal.

This first analytical-based estimate of the full waveform (for the equal-mass case, i.e. $\nu = \frac{1}{4}$ where $\nu \equiv \mu/M = m_1 m_2/(m_1+m_2)^2$) was given in Fig. 12 of [88] which is reproduced as Fig. 5 below. Note that the latter complete EOB waveform comes out of the analytical EOB formalism as a prediction which did not need to use any input from numerical data (which, anyway, did not exist at the time; see below). In addition, the proposal of [88] led to the first computation-based estimates of the losses of energy and angular-momentum during a BBH coalescence, and thereby of the mass and spin of the final BH made from the merger of the BBH. [The signal-to-noise-ratio estimates for BBH GWs of the previous work [98] were based on optimistic guesstimates, without any detailed computational basis.] In particular, the dimensionless spin parameter $a_f = cS_f/GM_f^2$ of the final BH was predicted, from the pioneering EOB model of [88], to be $a_f \simeq 0.795$ in the equal-mass case. This prediction is somewhat coarse (it is 11.5 % larger than current Numerical Relativity results $a_f^{NR} \simeq 0.69$), but later work has shown that including more analytical information in the EOB calculation was giving analytical results much closer to Numerical Relativity results (see Ref. [99]).

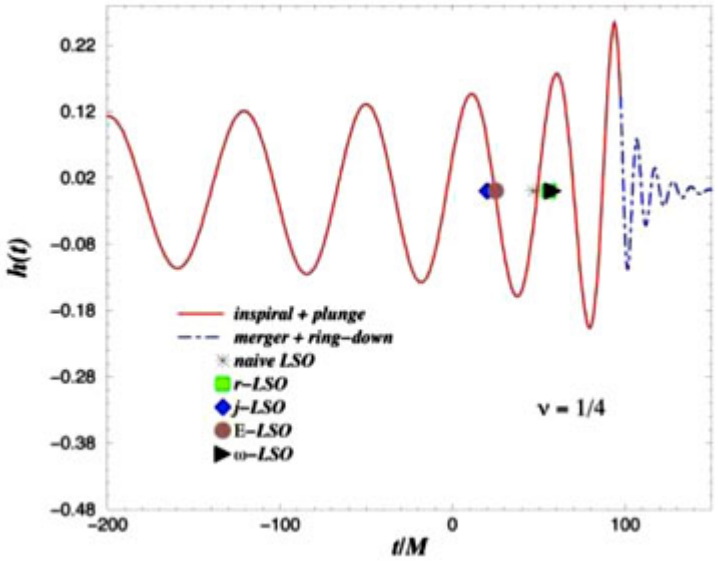

Figure 5: Fig. 12 of Ref. [88], i.e. "Plot of the complete waveform: inspiral and plunge followed by merger and ringdown", as obtained by completing the EOB Hamiltonian of [87] by a factorized and Padé-resummed radiation damping angular-momentum loss from [86], and a matched ringdown signal made of a (single, least-damped) quasi-normal mode of a Kerr black hole with mass and spin computed from the EOB formalim itself.

9 Numerical Relativity (NR) simulations of BBHs

Let us recall again that the matched-filter analysis, by the LIGO-Virgo collaboration, of candidate Gravitational Wave events from coalescing compact binaries used a large bank of precomputed of waveform templates. These templates were analytically constructed by combining Analytical Relativity (AR) information with Numerical Relativity (NR) information. Before describing the various ways in which AR and

NR information have been combined, let us briefly explain some of the theoretical aspects that enter NR simulations. In particular, we shall explain the mix of methods that enabled Frans Pretorius [100] to simulate (in a numerically stable manner), for the first time, in 2005 the last plunging orbit, leading to merger and ringdown, of a BBH, and to extract the corresponding waveform.

The *mathematical foundations* for NR were essentially contained, long ago, in papers of the French mathematical relativity school, notably Georges Darmois, André Lichnerowicz and Yvonne Choquet-Bruhat. Of particular importance was the work Ref. [101] by Yvonne Choquet-Bruhat, which proved the mathematical existence of local-in-time solutions to the harmonic-coordinates-reduced (vacuum) Einstein equations (which are diagonal-hyperbolic), and showed how to construct solutions of the full Einstein equations by then solving, on an initial Cauchy hypersurface, the harmonic-coordinates-version of the *constraints* of Einstein equations, and in proving that the constraints homogeneously propagate off the initial Cauchy hypersurface.

More precisely, the harmonic-coordinates condition used by Fourès-Bruhat (= Choquet-Bruhat) was of the form (in the following $a, b, \ldots = 0, 1, 2, 3$ denote spacetime indices)

$$C_a^{(0)} = 0 \tag{77}$$

where

$$C_a^{(0)} \equiv -g_{ab}\Box x^b \tag{78}$$

with

$$\Box x^a \equiv \frac{1}{\sqrt{g}}\partial_b\left(\sqrt{g}g^{bc}\partial_c x^a\right), \tag{79}$$

Then the harmonic-coordinates-reduced Einstein equations for the evolution of the spacetime metric g_{ab} read (Γ^c_{ab} denoting the usual Christoffel symbols)

$$\frac{1}{2}g^{cd}g_{ab,cd} + g^{cd}{}_{(,a}g_{b)d,c} + \Gamma^c_{bd}\Gamma^d_{ac} = -8\pi\left(T_{ab} - \frac{1}{2}g_{ab}T\right), \tag{80}$$

where T_{ab} is the stress-energy tensor of matter.

The diagonal-hyperbolic nature of the second-derivative term $\frac{1}{2}g^{cd}g_{ab,cd}$ allowed Fourès-Bruhat to prove the existence of local-in-time solutions of Eqs (80). To then get solutions of Einstein's original solutions one further needs to show how to satisfy, in addition, the conditions (77) everywhere in spacetime. The "constraints" $C^a_{(0)} \equiv g^{ab}C^{(0)}_b$ satisfy (when (80) are satisfied) the wave equation

$$\Box C^a_{(0)} = -R^a{}_b C^b_{(0)} \tag{81}$$

The latter propagation equation for the constraints is homogeneous. Therefore, if $C_a^{(0)}$, and their time-derivatives, vanish on some initial-time (Cauchy) hypersurface $t = x^0 = 0$ [which is shown to be related to the usual 3+1 hamiltonian and momentum constraints], they will continue to vanish for all times (as was correctly argued, and showed, by Fourès-Bruhat, back in 1952).

Besides the just explained harmonic-coordinates formulation of the Einstein equations, there exist many other ways of extracting an *evolution system* from Einstein's equations. As early as 1927, Georges Darmois [102] showed how, in Gauss

coordinates (i.e. $g_{00} = -1$ and $g_{0i} = 0$, or, equivalently $g^{00} = -1$ and $g^{0i} = 0$), Einstein's equations implied a second-order-in-time evolution system for the components of the spatial metric. The particular (and particularly simple) 3+1 decomposition of Einstein's equations obtained in Gauss (also called "synchronous") coordinates was later generalized to the general case where the values of g^{00} and g^{0i} are arbitrary. One can indeed use the four arbitrary functions entering a general coordinate transformation to give arbitrary values to the "lapse function" $\alpha \equiv (-g^{00})^{-\frac{1}{2}}$ and the "shift co-vector" $\beta_i = g_{0i}$. The Einstein equations, written as evolution equations for the time-development of the 3-metric γ_{ij}, in presence of arbitrary values of α and β_i are well-known [103, 68]. However, the latter "3+1" formulation(s) of Einstein's equations do not lead, in general, to evolution equations endowed with good properties (such as various forms of hyperbolicity behavior). One needs to complement them with adequate evolution equations for the lapse and the shift to end up with mathematically (and/or numerically) satisfactory evolution systems.

As explained above, the system obtained from writing Einstein equations in harmonic coordinates, i.e. Eqs. (80), define a mathematically satisfactory evolution system, in the sense that it is a diagonally-hyperbolic evolution system, for which theorems can be proved about the existence of solutions, given suitable initial (Cauchy) data. However, somewhat surprisingly, this evolution system was found to be *numerically unsatisfactory* on several accounts. First, the original harmonic-coordinate conditions can sometimes develop "cordinate pathologies" of their own. An in-principle remedy for avoiding such pathologies was advocated by Garfinkle [104]. It consists in generalizing the harmonic-coordinates condition $\Box x^a = 0$ to a generalized form $\Box x^a = H^a(x)$, where the $H^a(x)$ are some suitable "source functions". Such a generalization was earlier suggested by H. Friedrich [105] with a different motivation. One must then either specify the source functions $H^a(x)$ as explicit functions of the four spacetime coordinates, or give dynamical equations determining their evolution (and helping in avoiding coordinate pathologies). I shall not give here the equations that have been used to evolve the $H^a(x)$, because I mainly wish here to emphasize a *second* modification of the standard harmonic-coordinate approach that turned out to be a *crucial new ingredient* which allowed NR to succeed for the first time in 2005 to simulate the coalescence of BBH [100]. Indeed, it was found, before introducing this second modification, that the numerical evolution of Einstein's equations in generalized harmonic coordinates was generally numerically unstable, and does not allow to simulate the coalescence of two black holes.

When using Friedrich-Garfinkle *generalized harmonic coordinates* the constraints (77) are replaced by

$$C_a \equiv g_{ab} \left(H^a - \Box x^a \right) = 0. \tag{82}$$

Then, the crucial modification (used in [100]) of the correspondingly reduced Einstein equations consists in *adding extra terms proportional to the constraints* C_a in

Einstein's equations. Namely, Pretorius [100] considered now the evolution system

$$\frac{1}{2}g^{cd}g_{ab,cd} + \tag{83}$$

$$g^{cd}{}_{(,a}g_{b)d,c} + H_{(a,b)} - H_d\Gamma^d_{ab} + \Gamma^c_{bd}\Gamma^d_{ac} \tag{84}$$

$$+\kappa\left[n_{(a}C_{b)} - \frac{1}{2}g_{ab}n^dC_d\right] \tag{85}$$

$$= -8\pi\left(T_{ab} - \frac{1}{2}g_{ab}T\right). \tag{86}$$

Here, $n^a \equiv g^{ab}n_b$ denotes the unit timelike vector normal to the $t =$ const. hypersurfaces, and κ denotes an adjustable parameter.

One can then show that if the metric is evolved using (83-86), the constraints $C^a \equiv g^{ab}C_b$ will satisfy the following evolution equation

$$\Box C^a = -R^a{}_bC^b + 2\kappa\nabla_b\left[n^{(b}C^{a)}\right], \tag{87}$$

which generalizes (81). The crucial difference with respect to Eq. (81) is the presence of the last terms proportional to κ.

When κ is taken as being *positive* (and of an appropriate order of magnitude), the extra κ-dependent terms in the homogeneous evolution equation (87) tend to *damp* the evolution of the constraints C^a, i.e. they tend to make them tend exponentially towards zero when evolving them in the future of the initial Cauchy hypersurface. Because of this property, the extra terms (proportional to κC_a) added in the reduced Einstein equations (83-86) are called *constraint damping terms*.

The use of the extra constraint-damping terms was crucial to the breakthrough work of [100] in which to evolve, for the first time, a system of two black holes (initially formed by the collapse of a source T_{ab} made of a scalar field φ) was evolved, for the first time, through its last orbit, until coalescence and ringdown.

Before Pretorius, many authors had tackled the problem of the coalescence of BBH, but without succeeding in stably evolving two BHs on quasi-circular orbits. Besides the pioneering work of Smarr, and Eppley, around 1975 (head-on collision of two BHs starting from a small initial separation), one should cite the near breakthrough work, in 2004, of Bruegmann, Tichy and Jansen [106] (evolution of a BBH along one orbit). One should also mention that the idea of adding constraint-damping terms had surfaced in previous works, notably [107] and [108].

The GW waveform obtained in the first BBH coalescence simulation was given (in the form of the second time-derivative of the usual strain waveform, i.e. $\Psi_4 = \partial^2 h/\partial t^2$, this is why it looks different from the usually considered strain amplitude h, as discussed above) in Fig. 3 of [100], which is reproduced in Fig. 6 here.

The landmark paper [100] had a huge impact on the progress of the field of Numerical Relativity (NR). By showing that it was possible to concoct a suitable mix of methods allowing one to numerically simulate the coalescence of a BBH it gave to several other groups the motivation and energy to do the same.

On the one hand, the groups that followed on the heels of Pretorius in succeeding to numerically simulate BBH coalescence, namely [109] and [110], *did not use the same mix of methods* as Pretorius. They used instead a new trick consisting in allowing the two "punctures" representing the two BHs (introduced, and used earlier,

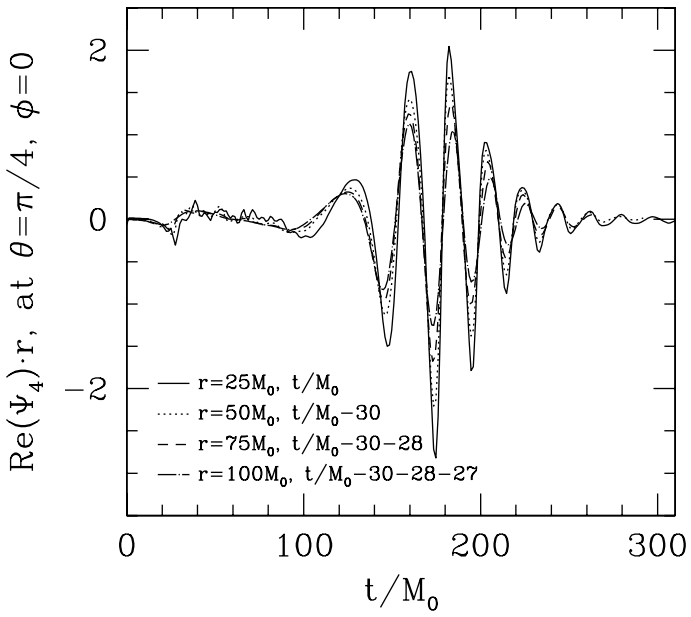

Figure 6: Fig. 3 of [100], i.e. "A sample of the gravitational waves emitted during the merger, as estimated by the Newman-Penrose scalar $\Psi_4[= \partial^2 h/\partial t^2]$ (from the medium resolution simulation). Here, the real component of Ψ_4 multiplied by the coordinate distance r from the center of the grid is shown at a fixed angular location, though several distances r."

by Brandt and Bruegmann) to move across the numerical grid (without the need of the BH horizon-excision method used by Pretorius). They also used a different formulation of the Einstein equations going under the name of BSSN, for Baumgarte-Shapiro-Shibata-Nakamura.

On the other hand, the Caltech-Cornell group, which has since then established itself as the indispensable provider of accurate BBH waveforms for LIGO, *did use a mix of methods comparable to the Pretorius one*, with generalized harmonic coordinates, excision, and, a *constraint-damping* method similar to the one used in [100]. The Caltech-Cornell Spectral code (nicknamed SPEC) was constructed in a sequence of works, and notably in Refs. [111], [112], and [113].

10 Combining Analytical Relativity (AR) with Numerical Relativity (NR) results for constructing accurate GW templates

Soon after the first numerical simulation of a BBH coalescence, Buonanno, Cook and Pretorius [114]: (i) extracted the main physical characteristics of the dynamics and GW emission of the last few orbits and of the merger of a BBH; and (ii) compared the results of their NR simulations to "analytical predictions based on the adiabatic post-Newtonian (PN) and nonadiabatic resummed-PN models (effective-one-body and Padé models)." Their main conclusions concerning the point (ii) were that:

1. they confirmed the prediction of [88] that "to a good approximation the inspiral phase of the evolution is quasicircular, followed by a blurred, quasicircular plunge lasting for about $1 - 1.5$ GW cycles."

2. "For all models considered, 3PN and 3.5PN orders match the inspiral numer-

ical data the best" (thereby confirming the usefulness of all the high-accuracy PN work).

3. In their Fig. 21 (reproduced below as Fig. 7) they compared the NR and $\mathrm{EOB}_{3.5PN}$ predictions for both the GW frequency evolution through late inspiral and merger, and the $C_{22} = \partial^2 h_{22}/\partial t^2$ ($\ell m = 22$) multipolar waveform. Their results showed a good qualitative, and rather good quantitative, agreement between NR and the purely analytical EOB model of the time.

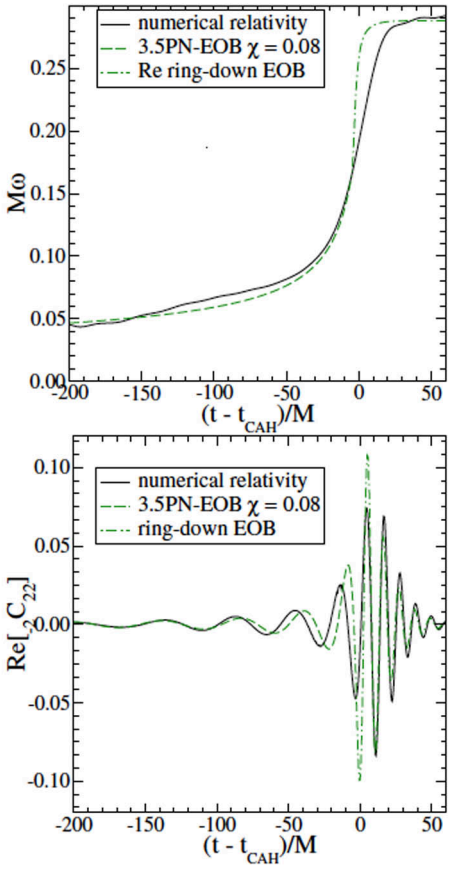

Figure 7: Fig. 21 of [114], i.e. the first NR/EOB comparison.

This qualitatively, and semi-quantitatively successful comparison between NR and EOB motivated several authors to extract (as had been earlier suggested in [135]) non-perturbative information from NR simulations and to incorporate it in the (at the time purely analytical) EOB formalism so as to improve the EOB-computed waveforms. This avenue of research was independently pursued by two groups: a group in France (around T. Damour), and a group in the US (around A. Buonanno). This effort led to the current extremely accurate NR-completed EOB waveforms, that we shall call EOB[NR] waveforms in the following. The construction of accurate EOB[NR] waveforms has been based on two pillars: (i) several improvements in EOB theory (notably the factorized, resummed waveform, see below); and (ii) extraction of non-perturbative strong-field information from NR simulations.

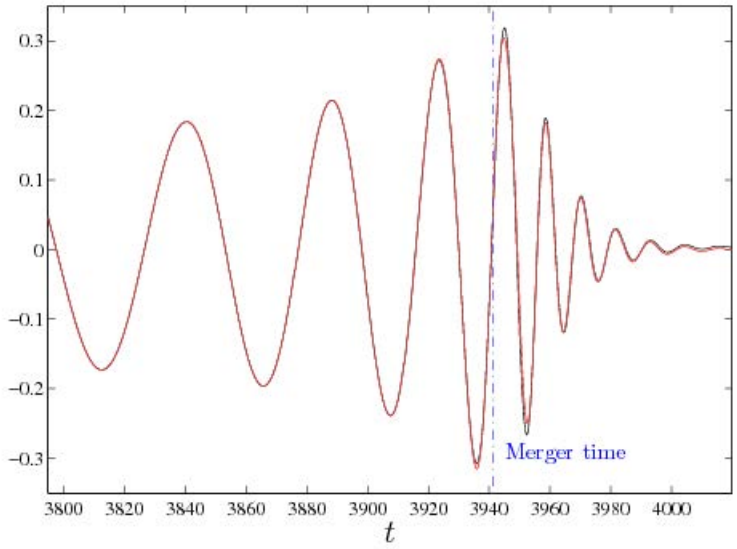

Figure 8: Fig. 1 of [93], i.e. "Equal-mass case: agreement between NR (black online) and EOB-based (red online) $\ell m = 22$ metric waveforms".

10.1 Improved resummation of the emitted radiation, and of radiation reaction

Several methods have been tried during the development of the EOB formalism to resum the radiation reaction $\widehat{\mathcal{F}}_\varphi$ (starting from the high-order PN-expanded results that have been obtained in the literature). Here, we shall briefly explain the *parameter-free* resummation technique for the multipolar waveform (and thus for the energy flux) introduced in Ref. [116, 115] and perfected in [92]. To be precise, the new results discussed in Ref. [92] are twofold: on the one hand, that work generalized the $\ell = m = 2$ resummed factorized waveform of [116, 115] to higher multipoles by using the most accurate currently known PN-expanded results [30, 117, 118, 119] as well as the higher PN terms which are known in the test-mass limit [120, 121]; on the other hand, it introduced a *new resummation procedure* which consists in considering a new theoretical quantity, denoted as $\rho_{\ell m}(x)$, which enters the (ℓ, m) waveform (together with other building blocks, see below) only through its ℓ-th power: $h_{\ell m} \propto (\rho_{\ell m}(x))^\ell$. Here, and below, x denotes the invariant PN-ordering parameter given during inspiral by $x \equiv (GM\Omega/c^3)^{2/3}$.

The main novelty introduced by Ref. [92] is to write the (ℓ, m) multipolar waveform emitted by a circular nonspinning compact binary as the *product* of several factors, namely

$$h^{(\epsilon)}_{\ell m} = \frac{GM\nu}{c^2 R} n^{(\epsilon)}_{\ell m} c_{\ell+\epsilon}(\nu) x^{(\ell+\epsilon)/2} Y^{\ell-\epsilon,-m}\left(\frac{\pi}{2}, \Phi\right) \hat{S}^{(\epsilon)}_{\rm eff} T_{\ell m} e^{{\rm i}\delta_{\ell m}} \rho^\ell_{\ell m}. \tag{88}$$

Here ϵ denotes the parity of $\ell + m$ ($\epsilon = \pi(\ell + m)$), i.e. $\epsilon = 0$ for "even-parity" (mass-generated) multipoles ($\ell + m$ even), and $\epsilon = 1$ for "odd-parity" (current-generated) ones ($\ell + m$ odd); $n^{(\epsilon)}_{\ell m}$ and $c_{\ell+\epsilon}(\nu)$ are numerical coefficients; $\hat{S}^{(\epsilon)}_{\rm eff}$ is a μ-normalized effective source (whose definition comes from the EOB formalism);

$T_{\ell m}$ is a resummed version [116, 115] of an infinite number of "leading logarithms" entering the *tail effects* [122, 123]; $\delta_{\ell m}$ is a supplementary phase (which corrects the phase effects not included in the *complex* tail factor $T_{\ell m}$), and, finally, $(\rho_{\ell m})^{\ell}$ denotes the ℓ-th power of the quantity $\rho_{\ell m}$ which is the new building block introduced in [92]. We refer to the latter reference for details on the various factors entering Eq. (88). Let us only mention here the explicit expression of the tail factor $T_{\ell m}$ which resums an infinite number of "leading logarithms" entering the transfer function between the near-zone multipolar wave and the far-zone one,

$$T_{\ell m} = \frac{\Gamma(\ell + 1 - 2\mathrm{i}\hat{\hat{k}})}{\Gamma(\ell+1)} e^{\pi \hat{\hat{k}}} e^{2\mathrm{i}\hat{\hat{k}} \log(2kr_0)}, \tag{89}$$

where $r_0 = 2GM/\sqrt{e}$ and $\hat{\hat{k}} \equiv G H^{\rm real}_{\rm EOB} m\Omega$ and $k \equiv m\Omega$.

For extensions of the (non spinning) factorized waveform of [92] to the spinning case, see [126, 127, 128]. Note also that, besides adding some specifically EOB-type information, the factorized EOB waveform nourishes itself from high-order PN-expanded waveform computations, such as Ref. [119], together with higher-order test-mass ($\nu \to 0$) GW computations, such as Refs. [120, 121, 124, 125].

Several studies, both in the test-mass limit, $\nu \to 0$, and in the comparable-mass case, have shown that the resummed factorized (inspiral) EOB waveforms defined above provided remarkably accurate analytical approximations to the "exact" inspiral waveforms computed by numerical simulations. These resummed multipolar EOB waveforms are much closer (especially during late inspiral) to the exact ones than the standard PN-expanded waveforms given by a PN-correction factor of the usual "Taylor-expanded" form

$$\widehat{h}^{(\epsilon)\rm PN}_{\ell m} = 1 + c^{\ell m}_1 x + c^{\ell m}_{3/2} x^{3/2} + c^{\ell m}_2 x^2 + \dots$$

To illustrate the performance of the resummed factorized EOB waveform we reproduce in Fig. 8 here the Fig. 1 of [92]. This Figure is a comparison between a very accurate SPEC waveform (for equal-mass, non-spinning BBH) and a NR-completed EOB waveform (in which the 5PN-level coefficient $a_6(\nu)$ in the EOB $A(u;\nu)$ potential was NR-fitted, as well as some non-quasi-circular corrections to the $\ell m = 22$ waveform; see below). The agreement between the red (EOB) and black (NR) curves is remarkably good (they are superposed nearly everywhere, except just after merger).

In addition, one uses the resummed multipolar waveforms (88) to define a resummation of the *radiation reaction force* $\mathcal{F}_\varphi$ defined as

$$\mathcal{F}_\varphi = -\frac{1}{\Omega} F^{(\ell_{\rm max})}, \tag{90}$$

where the (instantaneous, circular) GW flux $F^{(\ell_{\rm max})}$ is defined as

$$F^{(\ell_{\rm max})} = \frac{2}{16\pi G} \sum_{\ell=2}^{\ell_{\rm max}} \sum_{m=1}^{\ell} (m\Omega)^2 |R h_{\ell m}|^2. \tag{91}$$

11 EOB description of the merger of binary black holes and of the ringdown of the final black hole

Up to now we have reviewed how the EOB formalism, starting only from *analytical* information obtained from PN theory, and adding extra resummation requirements (both for the EOB conservative potentials A, Eq. (70), and D, and for the waveform, Eq. (88), and its associated radiation reaction force, Eqs. (90), (91)) makes specific predictions, both for the motion and the radiation of binary black holes. The analytical calculations underlying such an EOB description are essentially based on skeletonizing the two black holes as two, sufficiently separated point masses, and therefore seem unable to describe the merger of the two black holes, and the subsequent ringdown of the final, single black hole formed during the merger. However, as early as 2000 [**?**], the EOB formalism went one step further and proposed a specific strategy for describing the *complete* waveform emitted during the entire coalescence process, covering inspiral, merger and ringdown. This EOB proposal is somewhat crude. However, the predictions it has made (years before NR simulations could accurately describe the late inspiral and merger of binary black holes) have been broadly confirmed by subsequent NR simulations. Essentially, the EOB proposal (which was motivated partly by the closeness between the 2PN-accurate effective metric $g^{\rm eff}_{\mu\nu}$ [87] and the Schwarzschild metric, and by the results of Refs. [16] and [94]) consists of:

(i) defining, within EOB theory, the instant of (effective) "*merger*" of the two black holes as the (dynamical) EOB time t_m where the orbital frequency $\Omega(t)$ reaches its *maximum*;

(ii) describing (for $t \leq t_m$) the inspiral-plus-plunge (or simply *insplunge*) waveform, $h^{\rm insplunge}(t)$, by using the inspiral EOB dynamics and waveform reviewed in the previous Section; and

(iii) describing (for $t \geq t_m$) the merger-plus-ringdown waveform as a superposition of several quasi-normal-mode (QNM) complex frequencies of a final Kerr black hole (of mass M_f and spin parameter a_f, self-consistency estimated within the EOB formalism), say

$$\left(\frac{Rc^2}{GM}\right) h^{\rm ringdown}_{\ell m}(t) = \sum_N C^+_N \, e^{-\sigma^+_N (t-t_m)} \,, \tag{92}$$

with $\sigma^+_N = \alpha_N + i\,\omega_N$, and where the label N refers to indices (ℓ, ℓ', m, n), with (ℓ, m) being the Schwarzschild-background multipolarity of the considered (metric) waveform $h_{\ell m}$, with $n = 0, 1, 2 \ldots$ being the 'overtone number' of the considered Kerr-background Quasi-Normal-Mode, and ℓ' the degree of its associated spheroidal harmonics $S_{\ell' m}(a\sigma, \theta)$;

(iv) determining the excitation coefficients C^+_N of the QNM's in Eq. (92) by using a simplified representation of the transition between plunge and ring-down obtained by smoothly *matching* (following Ref. [116]), on a $(2p+1)$-toothed "comb" $(t_m - p\delta, \ldots, t_m - \delta, t_m, t_m + \delta, \ldots, t_m + p\delta)$ centered around the merger (and matching) time t_m, the inspiral-plus-plunge waveform to the above ring-down waveform.

Finally, one defines a complete, quasi-analytical EOB waveform (covering the full process from inspiral to ring-down) as:

$$h^{\rm EOB}_{\ell m}(t) = \theta(t_m - t)\, h^{\rm insplunge}_{\ell m}(t) + \theta(t - t_m)\, h^{\rm ringdown}_{\ell m}(t) \,, \tag{93}$$

where $\theta(t)$ denotes Heaviside's step function. The final result is a waveform that essentially depends only on the choice of a resummed EOB $A(u)$ potential, and, less importantly, on the choice of resummation of the main waveform amplitude factor $f_{22} = (\rho_{22})^2$.

12 NR-completed EOB templates (EOB[NR])

We have emphasized here that the EOB formalism is able, in principle, starting only from the best currently known analytical information, to predict the full waveform emitted by coalescing binary black holes. The early comparisons between 3PN-accurate EOB predicted waveforms[8] and NR-computed waveforms showed a satisfactory agreement between the two, within the (then relatively large) NR uncertainties [131, 132]. In addition, it has been shown that the Padé-resummed 3PN-accurate $A(u)$ potential is able, as is, to describe with remarkable accuracy several aspects of the dynamics of coalescing binary black holes, [133, 134].

On the other hand, when NR started delivering high-accuracy waveforms, it became clear that the 3PN-level analytical knowledge incorporated in EOB theory was not accurate enough for providing waveforms agreeing with NR ones within the high-accuracy needed for detection, and data analysis of upcoming GW signals. [See, *e.g.*, the discussion in Section II of Ref. [127].] At that point, one made use of the *natural flexibility* of the EOB formalism. Indeed, as already emphasized in early EOB work [28, 135], we know from the analytical point of view that there are (yet uncalculated) further terms in the u-expansions of the EOB potentials $A(u), D(u), \ldots$ (and in the x-expansion of the waveform), so that these terms can be introduced either as "free parameter(s) in constructing a bank of templates, and [one should] wait until" GW observations determine their value(s) [28], or as "*fitting parameters* and adjusted so as to reproduce other information one has about the exact results" (to quote Ref. [135]). For instance, modulo logarithmic corrections that will be further discussed below, the Taylor expansion in powers of u of the main EOB potential $A(u)$ reads

$$A^{\rm Taylor}(u;\nu) = 1 - 2u + \widetilde{a}_3(\nu)u^3 + \widetilde{a}_4(\nu)u^4 + \widetilde{a}_5(\nu)u^5 + \widetilde{a}_6(\nu)u^6 + \ldots$$

where the 2PN and 3PN coefficients $\widetilde{a}_3(\nu) = 2\nu$ and $\widetilde{a}_4(\nu) = a_4\nu$ have been known since 2001, but where the 4PN, 5PN,... coefficients, $\widetilde{a}_5(\nu), \widetilde{a}_6(\nu), \ldots$ were not known at the time (the analytical value of $\widetilde{a}_5(\nu)$ has been determined in 2013 [36]). A first attempt was made in [135] to use numerical data (on circular orbits of corotating black holes) to fit for the value of a (single, effective) 4PN parameter of the simple form $\widetilde{a}_5(\nu) = a_5\nu$ entering a Padé-resummed 4PN-level A potential, *i.e.*

$$A^1_4(u; a_5, \nu) = P^1_4\left[A_{\rm 3PN}(u) + \nu a_5 u^5\right] . \tag{94}$$

This strategy was pursued in Ref. [136, 115] and many subsequent works. It was pointed out in Ref. [93] that the introduction of a further 5PN coefficient $\widetilde{a}_6(\nu) = a_6\nu$, entering a Padé-resummed 5PN-level A potential, *i.e.*

$$A^1_5(u; a_5, a_6, \nu) = P^1_5\left[A_{\rm 3PN}(u) + \nu a_5 u^5 + \nu a_6 u^6\right] , \tag{95}$$

[8] The new, resummed EOB waveform discussed above was not available at the time, so that these comparisons employed the coarser "Newtonian-level" EOB waveform $h^{(N,\epsilon)}_{22}(x)$.

helped in having a closer agreement with accurate NR waveforms. See Refs. [140] and [141] for two different updated determinations of the EOB A potential.

In addition, Refs. [116, 115] introduced another type of flexibility parameters of the EOB formalism: the non quasi-circular (NQC) parameters accounting for uncalculated modifications of the quasi-circular inspiral waveform presented above, linked to deviations from an adiabatic quasi-circular motion. These NQC parameters are of various types, and subsequent works [129, 130, 93, 137, 138, 127] have explored several ways of introducing them. They enter the EOB waveform in two separate ways. First, through an explicit, additional complex factor multiplying $h_{\ell m}$, *e.g.*

$$f_{\ell m}^{\rm NQC} = (1 + a_1^{\ell m} n_1 + a_2^{\ell m} n_2) \exp[i(a_3^{\ell m} n_3 + a_4^{\ell m} n_4)]$$

where the n_i's are dynamical functions that vanish in the quasi-circular limit (with n_1, n_2 being time-even, and n_3, n_4 time-odd). For instance, one usually takes $n_1 = (p_{r_*}/r\Omega)^2$. Second, through the (discrete) choice of the argument used during the plunge to replace the variable x of the quasi-circular inspiral argument.

For a given value of the symmetric mass ratio, and given values of the A-flexibility parameters $\widetilde{a}_5(\nu), \widetilde{a}_6(\nu)$ one can determine the values of the NQC parameters $a_i^{\ell m}$'s from accurate NR simulations of binary black hole coalescence (with mass ratio ν) by imposing, say, that the complex EOB waveform $h_{\ell m}^{\rm EOB}(t^{\rm EOB}; \widetilde{a}_5, \widetilde{a}_6; a_i^{\ell m})$ *osculates* the corresponding NR one $h_{\ell m}^{\rm NR}(t^{\rm NR})$ at their respective instants of "merger", where $t^{\rm EOB}_{\rm merger} \equiv t^{\rm EOB}_m$ was defined above (maximum of $\Omega^{\rm EOB}(t)$), while $t^{\rm NR}_{\rm merger}$ is defined as the (retarded) NR time where the modulus $|h_{22}^{\rm NR}(t)|$ of the quadrupolar waveform reaches its maximum. The order of osculation that one requires between $h_{\ell m}^{\rm EOB}(t)$ and $h_{\ell m}^{\rm NR}(t)$ (or, separately, between their moduli and their phases or frequencies) depends on the number of NQC parameters $a_i^{\ell m}$. For instance, $a_1^{\ell m}$ and $a_2^{\ell m}$ affect only the modulus of $h_{\ell m}^{\rm EOB}$ and allow one to match both $|h_{\ell m}^{\rm EOB}|$ and its first time derivative, at merger, to their NR counterparts, while $a_3^{\ell m}, a_4^{\ell m}$ affect only the phase of the EOB waveform, and allow one to match the GW frequency $\omega_{\ell m}^{\rm EOB}(t)$ and its first time derivative, at merger, to their NR counterparts. The above EOB/NR matching scheme has been developed and declined in various versions in Refs. [129, 130, 93, 137, 138, 139, 127, 142]. One has also extracted the needed matching data from accurate NR simulations, and provided explicit, analytical ν-dependent fitting formulas for them [93, 127, 142]. The EOB/NR comparison displayed in Fig. 8 above used such an NR-completed EOB waveform.

As EOB waveforms are much faster to compute than NR waveforms[9], LIGO has used several banks of EOB[NR] templates (corresponding to different versions of spinning EOB[NR] models developed by the group of A. Buonanno [140]) for their search and data analysis pipelines. The spinning EOB[NR] (or SEOBNR) models used in the first searches used the further simplifying approximation of nonprecessing spin vectors (orthogonal to the orbital plane). [This approximation has been shown to be sufficient [144].] As a consequence, these EOB[NR] templates depend on four parameters: the two masses m_1, m_2 and the two algebraic spin magnitudes S_1, S_2. In view of the known properties of Kerr BHs, the latter are replaced by the dimensionless spin parameters $\chi_1 \equiv cS_1/Gm_1^2, \chi_2 \equiv cS_2/Gm_2^2$ which satisfy $-1 \leq \chi_a \leq +1$. [A positive (respectively, negative) value of χ corresponds to a spin vector aligned (respectively, antialigned) with respect to the orbital angular

[9] It takes more than a month to compute a reasonably long and accurate NR waveform.

momentum.] In principle, the four parameters m_1, m_2, χ_1, χ_2 vary continuously. In practice, one discretizes the four parameters to build an adequately dense bank of 250 000 waveforms covering the space of expected physical parameters (up to BH masses equal to $100M_\odot$). In addition, though the analytically-defined time-domain EOB[NR] templates take only minutes to be computed[10], the online searches, as well as the use of Bayesian methods, require the fast computation of many overlaps Eq. (26). To meed these demands, parametrized,"Reduced Order" Fourier-domain versions of the spinning EOB[NR] have been obtained [143]. To give an idea of the waveform template bank used in GW searches, we reproduce in Fig. 9 the Fig. 1 of [144], namely the projection on the $m_1 - m_2$ plane of the 250 000 bank of spinning EOB[NR] templates used by the LIGO-Virgo collaboration in their searches and data analysis. Note the circle which locates the position of the first discovered GW event: GW150914.

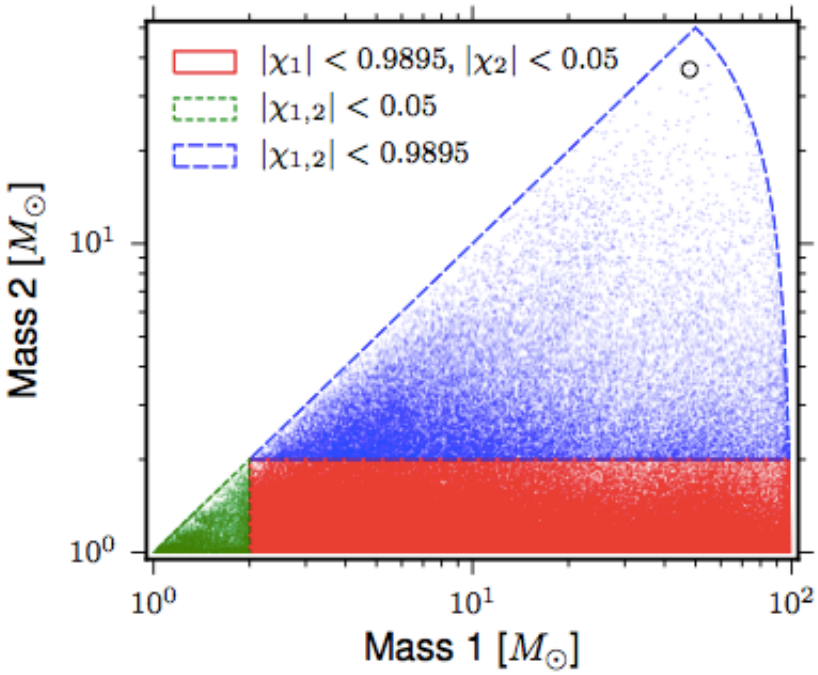

Figure 9: Fig. 1 of [144] showing the projection on the on the $m_1 - m_2$ plane (with the convention $m_1 \geq m_2$) of the 250 000 bank of spinning EOB[NR] templates used by the LIGO-Virgo collaboration in their searches and data analysis.

After the matched-filter analysis has extracted a BBH coalescence signal from the noisy data (and has established its significance by measuring in various ways the corresponding signal-to-noise-ratio, and false alarm probability), a more refined determination of the source parameters (masses and spins) is conducted by means of a coherent Bayesian analysis of source parameters, using locally denser banks of waveform templates. Two different such banks of templates have been used: one is made of spinning EOB[NR] templates (constructed as explained above), and the

[10]The EOB formalism defines, for each value of the masses and spins, a time-domain waveform via an analytical system of ODEs that needs to be numerically integrated.

other one is made of phenomenological versions [145] of wavefom EOB + NR hybrid templates constructed by joining together, in the time-domain, an EOB waveform describing the BBH inspiral to an NR waveform describing the last orbits and the merger of a BBH; the so-constructed bank of hybrid EOB + NR templates is then Fourier-transformed, and its Fourier-transform is encoded within a parametrized analytical representation; see Refs.[146] and [147].

13 The first discoveries

The two LIGO detectors have simultaneously observed, during the first run of advanced LIGO, two (and probably three) transient signals that can be confidently interpreted as GWs emitted by the coalescence of BBHs: GW150914 [1], GW151226 [2], and, with less confidence: LVT151012 [144]. Let us end by a few comments concerning these events.

13.1 GW150914

The values of the BH masses for the first GW event GW150914 were found to be larger than usually assumed for stellar BHs, namely:

$$m_1 = 36^{+5}_{-4} M_\odot \, ; \, m_1 = 29^{+4}_{-4} M_\odot \, ; \chi_{\rm eff} = -0.06^{+0.17}_{-0.18} \, . \tag{96}$$

Here, the last entry is the mass-weighted dimensionless spin parameter $(m_1\chi_1 + m_2\chi_2)/(m_1 + m_2)$. Its smallness suggests that the BHs were slowly spinning.

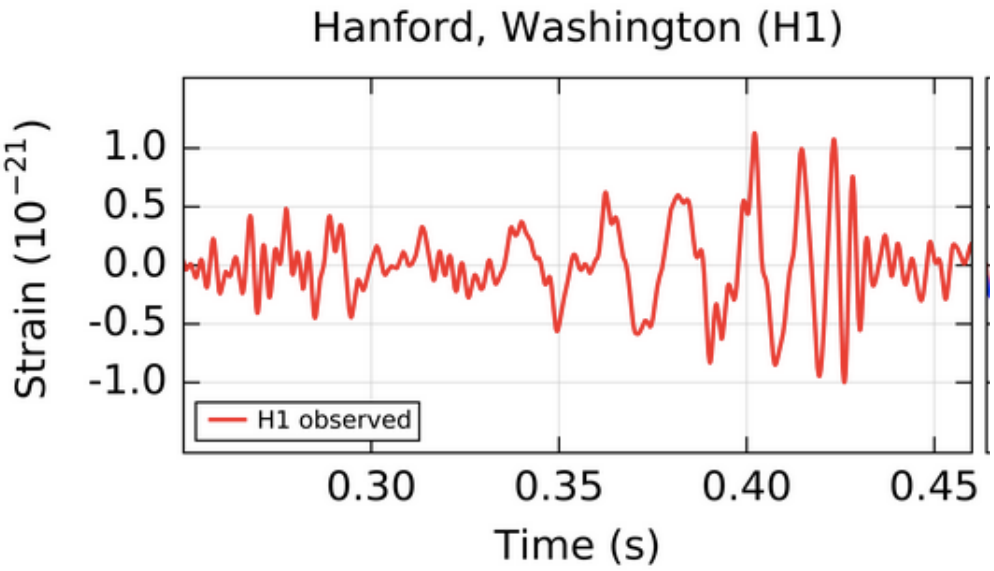

Figure 10: Adequately frequency-filtered output of the Hanford LIGO detector during the GW150914 event; from the upper left panel of Fig. 1 of [1]

This first event was so "loud" that a relatively simple filtering (combining a low-frequency filter, a high-frequency one, and the elimination of several discrete frequencies of oscillation) allowed the LIGO-Virgo collaboration to display a filtered

version of the detector's outputs in which one could recognize the theoretically predicted signal. Compare Fig. 10 to the originally predicted EOB waveform, Fig. 5 above, and to the corresponding improved EOB[NR] template directly computed from the best-fit values (96), which is displayed in Fig. 11 below

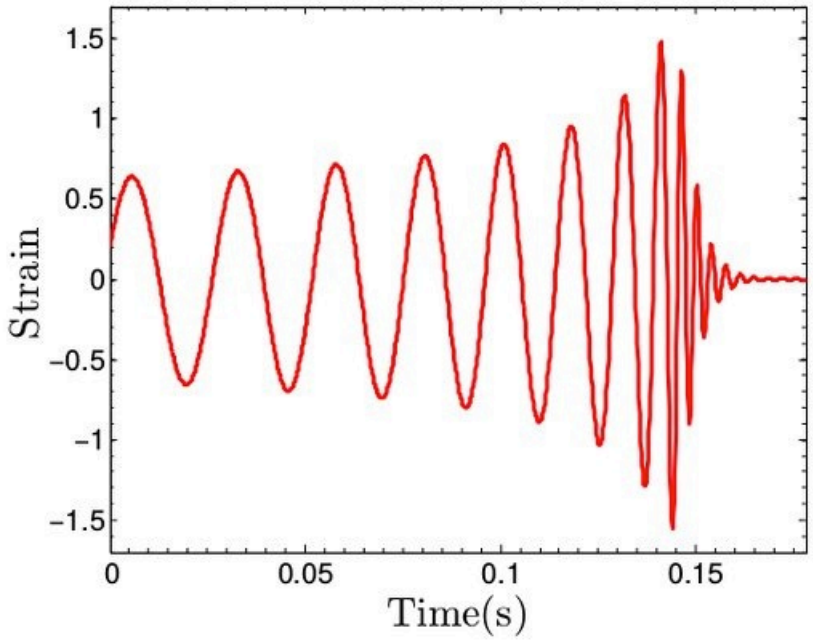

Figure 11: EOB[NR] BBH coalescence waveform computed with the EOB model of [141], using the best-fit parameters (96)

We wish, however, to emphasize that even for this remarkable event, the main contributions to the final, large (coherent) matched-filter squared signal-to-noise-ratio ($\rho^2 \approx (24)^2$) came from the latish inspiral, rather than from the merger. This is illustrated in Fig. 12 which displays the density per octave of frequency of squared signal-to-noise-ratio, i.e. $d\rho^2/d\ln f$, for GW150914. Indeed, the maximum of $d\rho^2/d\ln f$ occurs around 40 Hz, i.e. before the (EOB-predicted) Last Stable Orbit (LSO) [dot-dashed vertical line] which occurs at 67.65 Hz.

13.2 GW151226

The values of the BH masses for the first GW event GW151226 were found to be closer to the ones usually assumed for stellar BHs, namely:

$$m_1 = 14.2^{+8.3}_{-3.7} M_\odot \,;\, m_1 = 7.5^{+2.3}_{-2.3} M_\odot \,;\, \chi_{\rm eff} = +0.21^{+0.20}_{-0.10} \,. \tag{97}$$

In that case, the lower masses implies that the squared signal-to-noise-ratio was mainly accumulated during about 50 cycles before the merger, with relatively little contribution to the signal coming from the merger. The theoretical EOB[NR] waveform corresponding to the parameters (97) is displayed in Fig. 13, while the

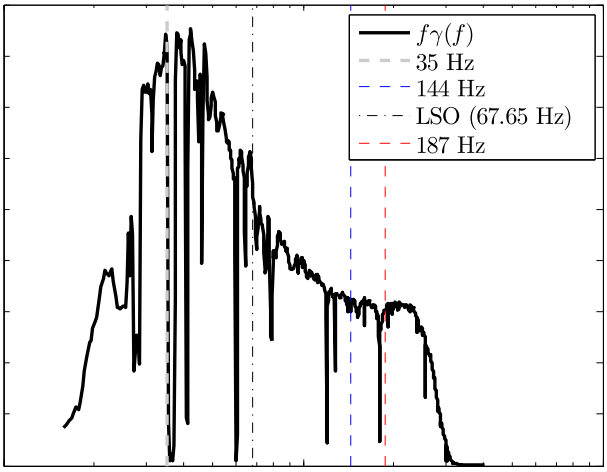

Figure 12: Density per octave of frequency of squared signal-to-noise-ratio, $d\rho^2/d\ln f$, for GW150914.

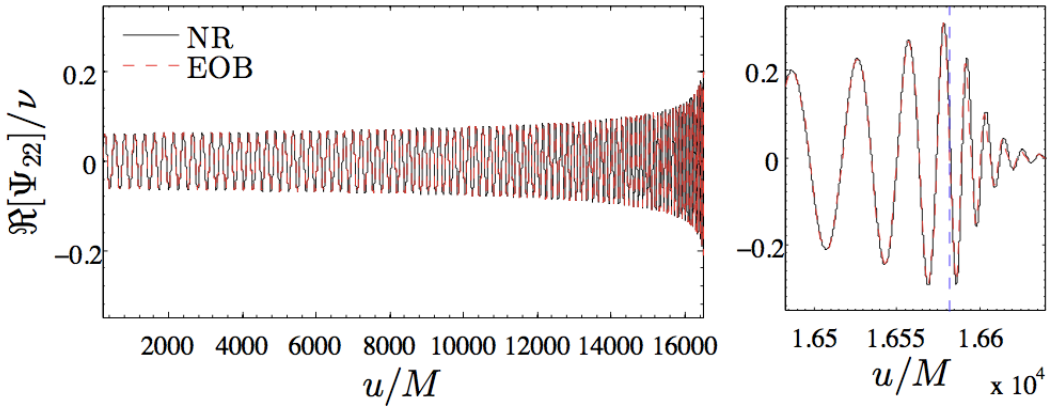

Figure 13: EOB[NR] BBH coalescence waveform computed with the EOB model of [141], using the best-fit parameters (97)

density of squared signal-to-noise-ratio $d\rho^2/d\ln f$ (which now shows no significant contribution from merger) is displayed in Fig. 14.

14 Conclusions

The momentous first detection, by the two LIGO interferometers, of transient gravitational wave signals, and their interpretation in terms of inspiralling and coalescing binary black holes has been significantly helped by many theoretical works. In particular, the many-year post-Newtonian-based analytical studies of the gravitational motion and radiation of binary black holes, followed by their resummed reformulation and extension within the Effective-One-Body formalism, and completed by extracting strong-field information from some numerical simulations, has been of crucial importance in allowing one to have in hands a large bank of waveform tem-

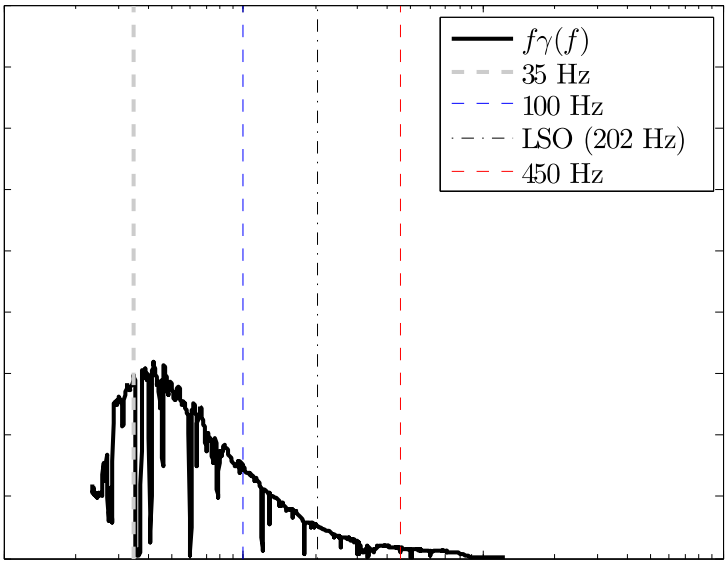

Figure 14: Density per octave of frequency of squared signal-to-noise-ratio, $d\rho^2/d\ln f$, for GW151226.

plates. The latter (Effective-One-Body-Numerical-Relativity) templates have been used both in the search and the data analysis of the first gravitatioal wave signals.

A new astronomy is born, and many exciting discoveries lie ahead, such as: gravitational wave signals from coalescing binary neutron stars, or from mixed black-hole-neutron-star systems, a possible cosmological background of gravitational waves, gravitational wave bursts from cusps and kinks on cosmic-size strings, etc.

References

[1] B. P. Abbott *et al.* [LIGO Scientific and Virgo Collaborations], "Observation of Gravitational Waves from a Binary Black Hole Merger," Phys. Rev. Lett. **116**, no. 6, 061102 (2016) [arXiv:1602.03837 [gr-qc]].

[2] B. P. Abbott *et al.* [LIGO Scientific and Virgo Collaborations], "GW151226: Observation of Gravitational Waves from a 22-Solar-Mass Binary Black Hole Coalescence," Phys. Rev. Lett. **116**, no. 24, 241103 (2016) [arXiv:1606.04855 [gr-qc]].

[3] A. Einstein, L. Infeld and B. Hoffmann, Ann. Math. **39**, 65-100 (1938).

[4] H.A. Lorentz and J. Droste, Versl. K. Akad. Wet. Amsterdam **26**, 392 (1917); and **26**, 649 (1917).

[5] A. Einstein, "Über Gravitationswellen," Sitzungsber. Preuss. Akad. Wiss. Berlin (Math. Phys.) **1918**, 154 (1918).

[6] L. D. Landau and E. M. Lifshitz, Course of Theoretical Physics. Vol. 2: Classical Field Theory, first Russian edition: 1941

[7] V.A. Fock, The Theory of Space, Time and Gravitation (Russian edition, Moscow, State Technical Publications, 1955)

[8] Freeman J. Dyson, "Gravitational Machines," in A.G.W. Cameron, ed., Interstellar Communication, New York: Benjamin Press, 1963, Chapter 12.

[9] P. C. Peters, "Gravitational Radiation and the Motion of Two Point Masses," Phys. Rev. **136**, B1224 (1964).

[10] P. C. Peters and J. Mathews, "Gravitational radiation from point masses in a Keplerian orbit," Phys. Rev. **131**, 435 (1963).

[11] K. Schwarzschild, "On the gravitational field of a mass point according to Einstein's theory," Sitzungsber. Preuss. Akad. Wiss. Berlin (Math. Phys.) **1916**, 189 (1916) [physics/9905030].

[12] R. P. Kerr, "Gravitational field of a spinning mass as an example of algebraically special metrics," Phys. Rev. Lett. **11**, 237 (1963).

[13] J. R. Oppenheimer and H. Snyder, "On Continued gravitational contraction," Phys. Rev. **56**, 455 (1939).

[14] C. V. Vishveshwara, "Scattering of Gravitational Radiation by a Schwarzschild Black-hole," Nature **227**, 936 (1970).

[15] W. H. Press, "Long Wave Trains of Gravitational Waves from a Vibrating Black Hole," Astrophys. J. **170**, L105 (1971).

[16] M. Davis, R. Ruffini and J. Tiomno, "Pulses of gravitational radiation of a particle falling radially into a schwarzschild black hole," Phys. Rev. D **5**, 2932 (1972).

[17] C. Cutler *et al.*, "The Last three minutes: issues in gravitational wave measurements of coalescing compact binaries," Phys. Rev. Lett. **70**, 2984 (1993) [astro-ph/9208005].

[18] T. Damour and N. Deruelle, "Radiation Reaction and Angular Momentum Loss in Small Angle Gravitational Scattering," Phys. Lett. A **87**, 81 (1981).

[19] T. Damour; Problème des deux corps et freinage de rayonnement en relativité générale. 1982. C.R. Acad. Sc. Paris, Série II, **294**, pp 1355-1357.

[20] T. Damour; Gravitational radiation and the motion of compact bodies. 1983. in *Gravitational Radiation*, edited by N. Deruelle and T. Piran, North-Holland, Amsterdam, pp 59-144.

[21] S.M. Kopeikin, Astron. Zh. **62**, 889 (1985).

[22] G. Schaefer, "The Gravitational Quadrupole Radiation Reaction Force and the Canonical Formalism of ADM," Annals Phys. **161**, 81 (1985).

[23] T. Ohta, H. Okamura, T. Kimura and K. Hiida, "Physically acceptable solution of einstein's equation for many-body system," Prog. Theor. Phys. **50**, 492 (1973).

[24] H. Okamura, T. Ohta, T. Kimura and K. Hiida, "Perturbation calculation of gravitational potentials," Prog. Theor. Phys. **50**, 2066 (1973).

[25] T. Ohta, H. Okamura, T. Kimura and K. Hiida, "Coordinate Condition and Higher Order Gravitational Potential in Canonical Formalism," Prog. Theor. Phys. **51**, 1598 (1974).

[26] Jaranowski, P. and Schäfer, G., "3rd post-Newtonian higher order Hamilton dynamics for two-body point-mass systems ([Erratum-ibid. D **63**, 029902 (2001)])", *Phys. Rev. D*, **57**, 72–74, (1998). [http://arxiv.org/abs/gr-qc/9712075gr-qc/9712075].

[27] Blanchet, L. and Faye, G., "General relativistic dynamics of compact binaries at the third post-Newtonian order", *Phys. Rev. D*, **63**, 062005, (2001). [http://arxiv.org/abs/gr-qc/0007051gr-qc/0007051].

[28] Damour, T., Jaranowski, P. and Schäfer, G., "Dimensional regularization of the gravitational interaction of point masses", *Phys. Lett. B*, **513**, 147–155, (2001). [http://arxiv.org/abs/gr-qc/0105038gr-qc/0105038].

[29] Itoh, Y. and Futamase, T., "New derivation of a third post-Newtonian equation of motion for relativistic compact binaries without ambiguity", *Phys. Rev. D*, **68**, 121501, (2003). [http://arxiv.org/abs/gr-qc/0310028gr-qc/0310028].

[30] Blanchet, L., Damour, T., Esposito-Farèse, G. and Iyer, B.R., "Gravitational radiation from inspiralling compact binaries completed at the third post-Newtonian order", *Phys. Rev. Lett.*, **93**, 091101, (2004). [http://arxiv.org/abs/gr-qc/0406012gr-qc/0406012].

[31] Foffa, S. and Sturani, R., "Effective field theory calculation of conservative binary dynamics at third post-Newtonian order", *Phys. Rev. D*, **84**, 044031, (2011). [http://arxiv.org/abs/1104.1122 [gr-qc]1104.1122 [gr-qc]].

[32] B. R. Iyer and C. M. Will, "PostNewtonian gravitational radiation reaction for two-body systems," Phys. Rev. Lett. **70**, 113 (1993).

[33] P. Jaranowski and G. Schäfer, "Towards the 4th post-Newtonian Hamiltonian for two-point-mass systems," Phys. Rev. D **86**, 061503 (2012) [arXiv:1207.5448 [gr-qc]].

[34] S. Foffa and R. Sturani, "Dynamics of the gravitational two-body problem at fourth post-Newtonian order and at quadratic order in the Newton constant," Phys. Rev. D **87**, no. 6, 064011 (2013) [arXiv:1206.7087 [gr-qc]].

[35] P. Jaranowski and G. Schäfer, "Dimensional regularization of local singularities in the 4th post-Newtonian two-point-mass Hamiltonian," Phys. Rev. D **87**, 081503 (2013) [arXiv:1303.3225 [gr-qc]].

[36] D. Bini and T. Damour, "Analytical determination of the two-body gravitational interaction potential at the 4th post-Newtonian approximation," *Phys. Rev. D*, **87**, 121501(R), (2013) [arXiv:1305.4884 [gr-qc]].

[37] P. Jaranowski and G. Schäfer, "Derivation of local-in-time fourth post-Newtonian ADM Hamiltonian for spinless compact binaries," Phys. Rev. D **92**, no. 12, 124043 (2015) [arXiv:1508.01016 [gr-qc]].

[38] L. Bernard, L. Blanchet, A. Boh, G. Faye and S. Marsat, "Fokker action of nonspinning compact binaries at the fourth post-Newtonian approximation," Phys. Rev. D **93**, no. 8, 084037 (2016) [arXiv:1512.02876 [gr-qc]].

[39] T. Damour, P. Jaranowski and G. Schäfer, "Nonlocal-in-time action for the fourth post-Newtonian conservative dynamics of two-body systems," Phys. Rev. D **89**, no. 6, 064058 (2014) [arXiv:1401.4548 [gr-qc]].

[40] T. Damour, P. Jaranowski and G. Schäfer, "Fourth post-Newtonian effective one-body dynamics," Phys. Rev. D **91**, no. 8, 084024 (2015) [arXiv:1502.07245 [gr-qc]].

[41] T. Damour, P. Jaranowski and G. Schäfer, "Conservative dynamics of two-body systems at the fourth post-Newtonian approximation of general relativity," Phys. Rev. D **93**, no. 8, 084014 (2016) [arXiv:1601.01283 [gr-qc]].

[42] T. Damour, "The Problem Of Motion In Newtonian And Einsteinian Gravity," in *300 Years of Gravitation*, edited by S. W. Hawking and W. Israel (Cambride University press, Cambride, 1987), pp. 128-198.

[43] F. K. Manasse: J. Math. Phys. **4**, 746 (1963).

[44] M. Demianski and L. P. Grishchuk, "Note on the motion of black holes", Gen. Relat. Gravit. **5** 673 (1974)

[45] P. D. D'Eath: Phys. Rev. D **11**, 1387 (1975).

[46] R. E. Kates: Phys. Rev. D **22**, 1853 (1980).

[47] D. M. Eardley: Astrophys. J. **196**, L59 (1975).

[48] C. M. Will, D. M. Eardley: Astrophys. J. **212**, L91 (1977).

[49] T. Damour: *Gravitational radiation and the motion of compact bodies*, in Gravitational Radiation, edited by N. Deruelle and T. Piran, North-Holland, Amsterdam, pp. 59-144 (1983).

[50] K. S. Thorne and J. B. Hartle: Laws of motion and precession for black holes and other bodies, Phys. Rev. D **31**, 1815 (1984).

[51] C. M. Will: *Theory and experiment in gravitational physics*, Cambridge University Press (1993) 380 p.

[52] S.M. Kopeikin, Celestial Mechanics **44**, 87 (1988); V. A. Brumberg and S. M. Kopejkin: Nuovo Cimento B **103**, 63 (1988); S.A. Klioner and A.V. Voinov, Phys. Rev. D **48**, 1451 (1993).

[53] T. Damour, M. Soffel and C. M. Xu: General relativistic celestial mechanics. 1. Method and definition of reference system, Phys. Rev. D **43**, 3273 (1991); General relativistic celestial mechanics. 2. Translational equations of motion, Phys. Rev. D **45**, 1017 (1992); General relativistic celestial mechanics. 3. Rotational equations of motion, Phys. Rev. D **47**, 3124 (1993); General relativistic celestial mechanics. 4. Theory of satellite motion, Phys. Rev. D **49**, 618 (1994).

[54] G. 't Hooft and M. J. G. Veltman: Regularization and renormalization of gauge fields, Nucl. Phys. B **44**, 189 (1972).

[55] T. Damour, G. Esposito-Farèse: Gravitational-wave versus binary-pulsar tests of strong-field gravity, Phys. Rev. D **58**, 042001 (1998).

[56] W. D. Goldberger and I. Z. Rothstein, "An Effective field theory of gravity for extended objects," Phys. Rev. D **73**, 104029 (2006) doi:10.1103/PhysRevD.73.104029 [hep-th/0409156].

[57] L. Infeld and J. Plebański, *Motion and Relativity* (Pergamon, Oxford, 1960).

[58] T. Ohta, H. Okamura, K. Hiida, and T. Kimura, "Higher order gravitational potential for many-body system," Prog. Theor. Phys. **51**, 1220 (1974).

[59] T. Damour and G. Schäfer, "Lagrangians for n point masses at the second post-Newtonian approximation of general relativity," Gen. Relativ. Gravit. **17**, 879 (1985).

[60] T. Damour and G. Esposito-Farèse, "Tensor multiscalar theories of gravitation," Class. Quant. Grav. **9**, 2093 (1992).

[61] T. Damour and G. Esposito-Farèse, "Testing gravity to second post-Newtonian order: A field theory approach," Phys. Rev. D **53**, 5541 (1996) [gr-qc/9506063].

[62] K. Westpfahl and M. Goller, "Gravitational scattering of two relativistic particles in postlinear approximation," Lett. Nuovo Cim. **26**, 573 (1979).

[63] L. Bel, T. Damour, N. Deruelle, J. Ibañez, and J. Martin, "Poincaré invariant gravitational field and equations of motion of two point-like objects: The postlinear approximation of general relativity," Gen. Relativ. Gravit. **13**, 963 (1981).

[64] J. B. Gilmore and A. Ross, "Effective field theory calculation of second post-Newtonian binary dynamics," Phys. Rev. D **78**, 124021 (2008) [arXiv:0810.1328 [gr-qc]].

[65] Y.-Z. Chu, "The n-body problem in general relativity up to the second post-Newtonian order from perturbative field theory," Phys. Rev. D **79**, 044031 (2009) [arXiv:0812.0012 [gr-c]].

[66] S. Foffa and R. Sturani, "Effective field theory calculation of conservative binary dynamics at third post-Newtonian order," Phys. Rev. D **84**, 044031 (2011) [arXiv:1104.1122 [gr-qc]].

[67] P. Jaranowski and G. Schäfer, "Third post-Newtonian higher order ADM Hamilton dynamics for two-body point mass systems," Phys. Rev. D **57**, 7274 (1998); **63**, 029902(E) (2001) [gr-qc/9712075].

[68] R. Arnowitt, S. Deser, and C. W. Misner, in *Gravitation: An Introduction to Current Research*, edited by L. Witten (John Wiley, New York, 1962), p. 227 [gr-qc/0405109].

[69] L. Blanchet and T. Damour, "Tail Transported Temporal Correlations in the Dynamics of a Gravitating System," Phys. Rev. D **37**, 1410 (1988).

[70] G. Schäfer, "Acceleration-dependent lagrangians in general relativity," Phys. Lett. A **100**, 128 (1984).

[71] T. Damour and G. Schäfer, "Lagrangians forn point masses at the second post-Newtonian approximation of general relativity," Gen. Rel. Grav. **17**, 879 (1985).

[72] T. Damour and G. Schaefer, "Redefinition of position variables and the reduction of higher order Lagrangians," J. Math. Phys. **32**, 127 (1991).

[73] R. Epstein and R. V. Wagoner "Post-Newtonian generation of gravitational waves" Astrophysical Journal, **197**, 717-723 (1975)

[74] R. V. Wagoner and C. M. Will, "PostNewtonian Gravitational Radiation from Orbiting Point Masses," Astrophys. J. **210**, 764 (1976) Erratum: [Astrophys. J. **215**, 984 (1977)].

[75] C. M. Will and A. G. Wiseman, "Gravitational radiation from compact binary systems: Gravitational wave forms and energy loss to second postNewtonian order," Phys. Rev. D **54**, 4813 (1996) [gr-qc/9608012].

[76] L. Blanchet and T. Damour, "Radiative gravitational fields in general relativity I. general structure of the field outside the source," Phil. Trans. Roy. Soc. Lond. A **320**, 379 (1986).

[77] L. Blanchet and T. Damour, "Postnewtonian Generation of Gravitational Waves," Annales Poincare Phys. Theor. **50**, 377 (1989).

[78] T. Damour and B. R. Iyer, "Multipole analysis for electromagnetism and linearized gravity with irreducible cartesian tensors," Phys. Rev. D **43**, 3259 (1991).

[79] L. Blanchet, "Second postNewtonian generation of gravitational radiation," Phys. Rev. D **51**, 2559 (1995) [gr-qc/9501030].

[80] L. Blanchet, "On the multipole expansion of the gravitational field," Class. Quant. Grav. **15**, 1971 (1998) [gr-qc/9801101].

[81] L. Blanchet, T. Damour and B. R. Iyer, "Gravitational waves from inspiralling compact binaries: Energy loss and wave form to second postNewtonian order," Phys. Rev. D **51**, 5360 (1995) Erratum: [Phys. Rev. D **54**, 1860 (1996)] [gr-qc/9501029].

[82] L. Blanchet, T. Damour, G. Esposito-Farese and B. R. Iyer, "Gravitational radiation from inspiralling compact binaries completed at the third post-Newtonian order," Phys. Rev. Lett. **93**, 091101 (2004) [gr-qc/0406012].

[83] T. Damour and B. R. Iyer, "PostNewtonian generation of gravitational waves. 2. The Spin moments," Ann. Inst. H. Poincare Phys. Theor. **54**, 115 (1991).

[84] L. Blanchet, "Gravitational Radiation from Post-Newtonian Sources and Inspiralling Compact Binaries," arXiv:1310.1528 [gr-qc].

[85] P. R. Brady, J. D. E. Creighton and K. S. Thorne, "Computing the merger of black hole binaries: The IBBH problem," Phys. Rev. D **58**, 061501 (1998) doi:10.1103/PhysRevD.58.061501 [gr-qc/9804057].

[86] Damour, T., Iyer, B.R. and Sathyaprakash, B.S., "Improved filters for gravitational waves from inspiralling compact binaries", *Phys. Rev. D*, **57**, 885, (1998). [http://arxiv.org/abs/gr-qc/9708034gr-qc/9708034].

[87] A. Buonanno and T. Damour, "Effective one-body approach to general relativistic two-body dynamics," Phys. Rev. D **59**, 084006 (1999) [gr-qc/9811091].

[88] A. Buonanno and T. Damour, "Transition from inspiral to plunge in binary black hole coalescences," Phys. Rev. D **62**, 064015 (2000) [gr-qc/0001013].

[89] T. Damour, P. Jaranowski and G. Schaefer, "On the determination of the last stable orbit for circular general relativistic binaries at the third postNewtonian approximation," Phys. Rev. D **62**, 084011 (2000) [gr-qc/0005034].

[90] T. Damour, "Coalescence of two spinning black holes: an effective one-body approach," Phys. Rev. D **64**, 124013 (2001) [gr-qc/0103018].

[91] Brézin, E., Itzykson, C. and Zinn-Justin, J., "Relativistic balmer formula including recoil effects", *Phys. Rev. D*, **1**, 2349, (1970).

[92] Damour, T., Iyer, B.R. and Nagar, A., "Improved resummation of post-Newtonian multipolar waveforms from circularized compact binaries", *Phys. Rev. D*, **79**, 064004, (2009). [http://arxiv.org/abs/0811.2069 [gr-qc]0811.2069 [gr-qc]]

[93] Damour, T. and Nagar, A., "An improved analytical description of inspiralling and coalescing black-hole binaries", *Phys. Rev. D*, **79**, 081503, (2009). [http://arxiv.org/abs/0902.0136 [gr-qc]0902.0136 [gr-qc]].

[94] Price, R.H. and Pullin, J., "Colliding black holes: The Close limit", *Phys. Rev. Lett.*, **72**, 3297, (1994). [http://arxiv.org/abs/gr-qc/9402039gr-qc/9402039].

[95] Damour, T. and Schäfer, G., "Higher order relativistic periastron advances and binary pulsars", *Nuovo Cim. B*, **101**, 127, (1988).

[96] Damour, T., Jaranowski, P. and Schäfer, G., "Dynamical invariants for general relativistic two-body systems at the third postNewtonian approximation", *Phys. Rev. D*, **62**, 044024, (2000). [http://arxiv.org/abs/gr-qc/9912092gr-qc/9912092].

[97] T. Damour, P. Jaranowski, and G. Schäfer, "On the determination of the last stable orbit for circular general relativistic binaries at the third post-Newtonian approximation," Phys. Rev. D **62**, 084011 (2000) [gr-qc/0005034].

[98] E. E. Flanagan and S. A. Hughes, "Measuring gravitational waves from binary black hole coalescences: 1. Signal-to-noise for inspiral, merger, and ringdown," Phys. Rev. D **57**, 4535 (1998) [gr-qc/9701039].

[99] T. Damour and A. Nagar, "Final spin of a coalescing black-hole binary: An Effective-one-body approach," Phys. Rev. D **76**, 044003 (2007) [arXiv:0704.3550 [gr-qc]].

[100] F. Pretorius, "Evolution of binary black hole spacetimes," Phys. Rev. Lett. **95**, 121101 (2005) [gr-qc/0507014].

[101] Y. Fourès-Bruhat, "Theoreme d'existence pour certains systemes derivees partielles non lineaires," Acta Mat. **88**, 141 (1952).

[102] G. Darmois, Les quations de la gravitation einsteinienne, Mmorial des sciences mathmatiques, fascicule 25 (1927) pp1-48. [available on www.numdam]

[103] Y. Fourès-Bruhat "Sur l'intégration des équations de la Relativité Générale" J. Rat. Mech. and Anal. **5** 951-966 (1956)

[104] D. Garfinkle "Harmonic coordinate method for simulating generic singularities," Phys. Rev. D **65**, 044029 (2002) [gr-qc/0110013].

[105] H. Friedrich, Conformal Einstein evolution, Lect. Notes Phys. 604, 1 (2002)

[106] B. Bruegmann, W. Tichy and N. Jansen, "Numerical simulation of orbiting black holes," Phys. Rev. Lett. **92**, 211101 (2004) [gr-qc/0312112].

[107] O. Brodbeck, S. Frittelli, P. Hubner and O. A. Reula, "Einstein's equations with asymptotically stable constraint propagation," J. Math. Phys. **40**, 909 (1999) [gr-qc/9809023].

[108] C. Gundlach, J. M. Martin-Garcia, G. Calabrese and I. Hinder, "Constraint damping in the Z4 formulation and harmonic gauge," Class. Quant. Grav. **22**, 3767 (2005) [gr-qc/0504114].

[109] M. Campanelli, C. O. Lousto, P. Marronetti and Y. Zlochower, "Accurate evolutions of orbiting black-hole binaries without excision," Phys. Rev. Lett. **96**, 111101 (2006) [gr-qc/0511048].

[110] J. G. Baker, J. Centrella, D. I. Choi, M. Koppitz and J. van Meter, "Gravitational wave extraction from an inspiraling configuration of merging black holes," Phys. Rev. Lett. **96**, 111102 (2006) [gr-qc/0511103].

[111] L. Lindblom, M. A. Scheel, L. E. Kidder, R. Owen and O. Rinne, "A New generalized harmonic evolution system," Class. Quant. Grav. **23**, S447 (2006) [gr-qc/0512093].

[112] M. A. Scheel, H. P. Pfeiffer, L. Lindblom, L. E. Kidder, O. Rinne and S. A. Teukolsky, "Solving Einstein's equations with dual coordinate frames," Phys. Rev. D **74**, 104006 (2006) [gr-qc/0607056].

[113] L. Lindblom, K. D. Matthews, O. Rinne and M. A. Scheel, "Gauge Drivers for the Generalized Harmonic Einstein Equations," Phys. Rev. D **77**, 084001 (2008) [arXiv:0711.2084 [gr-qc]].

[114] A. Buonanno, G. B. Cook and F. Pretorius, "Inspiral, merger and ringdown of equal-mass black-hole binaries," Phys. Rev. D **75**, 124018 (2007) [gr-qc/0610122].

[115] Damour, T. and Nagar, A., "Comparing Effective-One-Body gravitational waveforms to accurate numerical data", *Phys. Rev. D*, **77**, 024043, (2008). [http://arxiv.org/abs/0711.2628 [gr-qc]0711.2628 [gr-qc]].

[116] Damour, T. and Nagar, A., "Faithful Effective-One-Body waveforms of small-mass-ratio coalescing black-hole binaries", *Phys. Rev. D*, **76**, 064028, (2007). [http://arxiv.org/abs/0705.2519 [gr-qc]0705.2519 [gr-qc]].

[117] Kidder, L.E., "Using Full Information When Computing Modes of Post-Newtonian Waveforms From Inspiralling Compact Binaries in Circular Orbit", *Phys. Rev. D*, **77**, 044016, (2008). [http://arxiv.org/abs/0710.0614 [gr-qc]0710.0614 [gr-qc]].

[118] Berti, E., Cardoso, V., Gonzalez, J.A., Sperhak, U., Hannam, M., Husa, S. and Bruegmann, B., "Inspiral, merger and ringdown of unequal mass black hole binaries: A multipolar analysis", *Phys. Rev. D*, **76**, 064034, (2007). [http://arxiv.org/abs/gr-qc/0703053gr-qc/0703053].

[119] Blanchet, L., Faye, G., Iyer, B.R. and Sinha, S., "The third post-Newtonian gravitational wave polarisations and associated spherical harmonic modes for inspiralling compact binaries in quasi-circular orbits", *Class. Quant. Grav.*, **25**, 165003, (2008). [http://arxiv.org/abs/0802.1249 [gr-qc]0802.1249 [gr-qc]].

[120] Tagoshi, H. and Sasaki, M., "Post-Newtonian Expansion of Gravitational Waves from a Particle in Circular Orbit around a Schwarzschild Black Hole", *Prog. Theor. Phys*, **92**, 745–771, (1994). [http://arxiv.org/abs/gr-qc/9405062gr-qc/9405062].

[121] Tanaka, T., Tagoshi, H. and Sasaki, M., "Gravitational Waves by a Particle in Circular Orbit around a Schwarzschild Black Hole", *Prog. Theor. Phys*, **96**, 1087–1101, (1996). [http://arxiv.org/abs/gr-qc/9701050gr-qc/9701050].

[122] Blanchet, L. and Damour, T., "Hereditary Effects In Gravitational Radiation", *Phys. Rev. D*, **46**, 4304, (1992).

[123] Blanchet, L., "Gravitational-wave tails of tails, [Erratum-ibid. **22**, 3381 (2005)]", *Class. Quant. Grav.*, **15**, 113, (1998). [http://arxiv.org/abs/gr-qc/9710038gr-qc/9710038].

[124] Fujita, R. and Iyer, B.R., "Spherical harmonic modes of 5.5 post-Newtonian gravitational wave polarisations and associated factorised resummed waveforms for a particle in circular orbit around a Schwarzschild black hole", *Phys. Rev. D*, **82**, 044051, (2010). [http://arxiv.org/abs/1005.2266 [gr-qc]1005.2266 [gr-qc]].

[125] Fujita, R., "Gravitational radiation for extreme mass ratio inspirals to the 14th post-Newtonian order", *Prog. Theor. Phys.*, **127**, 583, (2012). [http://arxiv.org/abs/1104.5615 [gr-qc]1104.5615 [gr-qc]].

[126] Pan, Y., Buonanno, A., Fujita, R., Racine, E. and Tagoshi, H., "Post-Newtonian factorized multipolar waveforms for spinning, non-precessing black-hole binaries", *Phys. Rev. D*, **83**, 064003, (2011). [http://arxiv.org/abs/1006.0431 [gr-qc]1006.0431 [gr-qc]].

[127] Pan, Y., Buonanno, A., Boyle, M., Buchman, L.T., Kidder, L.E., Pfeiffer, H.P. and Scheel, M.A., "Inspiral-merger-ringdown multipolar waveforms of nonspinning black-hole binaries using the effective-one-body formalism", *Phys. Rev. D*, **84**, 124052, (2011). [http://arxiv.org/abs/1106.1021 [gr-qc]1106.1021 [gr-qc]].

[128] Taracchini, A., Pan, Y., Buonanno, A., Barausse, E., Boyle, M., Chu, T., Lovelace, G. and Pfeiffer, H.P. *et al.*, "Prototype effective-one-body model for nonprecessing spinning inspiral-merger-ringdown waveforms", *Phys. Rev. D*, **86**, 024011, (2012). [http://arxiv.org/abs/1202.0790 [gr-qc]1202.0790 [gr-qc]].

[129] Damour, T., Nagar, A., Nils Dorband, E., Pollney, D. and Rezzolla, L., "Faithful Effective-One-Body waveforms of equal-mass coalescing black-hole binaries", *Phys. Rev. D*, **77**, 084017, (2008). [http://arxiv.org/abs/0712.3003 [gr-qc]0712.3003 [gr-qc]].

[130] Damour, T., Nagar, A., Hannam, M., Husa, S. and Bruegmann, B., "Accurate Effective-One-Body waveforms of inspiralling and coalescing black-hole binaries", *Phys. Rev. D*, **78**, 044039, (2008). [http://arxiv.org/abs/0803.3162 [gr-qc]0803.3162 [gr-qc]].

[131] Buonanno, A., Cook, G.B. and Pretorius, F., "Inspiral, merger and ringdown of equal-mass black-hole binaries", *Phys. Rev. D*, **75**, 124018, (2007). [http://arxiv.org/abs/gr-qc/0610122gr-qc/0610122].

[132] Pan, Y. *et al.*, "A data-analysis driven comparison of analytic and numerical coalescing binary waveforms: Nonspinning case", *Phys. Rev. D*, **77**, 024014, (2008). [http://arxiv.org/abs/0704.1964 [gr-qc]0704.1964 [gr-qc]].

[133] Le Tiec, A., Mroue, A.H., Barack, L., Buonanno, A., Pfeiffer, H.P., Sago, N. and Taracchini, A., "Periastron Advance in Black Hole Binaries", *Phys. Rev. Lett.*, **107**, 141101, (2011). [http://arxiv.org/abs/1106.3278 [gr-qc]1106.3278 [gr-qc]].

[134] Damour, T., Nagar, A., Pollney, D. and Reisswig, C., "Energy versus Angular Momentum in Black Hole Binaries", *Phys. Rev. Lett.*, **108**, 131101, (2012). [http://arxiv.org/abs/1110.2938 [gr-qc]1110.2938 [gr-qc]].

[135] Damour, T., Gourgoulhon, E. and Grandclément, P., "Circular orbits of corotating binary black holes: Comparison between analytical and numerical results", *Phys. Rev. D*, **66**, 024007, (2002). [http://arxiv.org/abs/gr-qc/0204011gr-qc/0204011].

[136] Buonanno, A., Pan, Y., Baker, J.G., Centrella, J., Kelly, B.J., McWilliams, S.T. and van Meter, J.R., "Toward faithful templates for non-spinning binary black holes using the effective-one-body approach", *Phys. Rev. D*, **76**, 104049, (2007). [http://arxiv.org/abs/0706.3732 [gr-qc]0706.3732 [gr-qc]].

[137] Buonanno, A., Pan, Y., Pfeiffer, H.P., Scheel, M.A., Buchman, L.T. and Kidder, L.E., "Effective-one-body waveforms calibrated to numerical relativity simulations: coalescence of non-spinning, equal-mass black holes", *Phys. Rev. D*, **79**, 124028, (2009). [http://arxiv.org/abs/0902.0790 [gr-qc]0902.0790 [gr-qc]].

[138] Bernuzzi, S., Nagar, A. and Zenginoglu, A., "Binary black hole coalescence in the extreme-mass-ratio limit: testing and improving the effective-one-body multipolar waveform", *Phys. Rev. D*, **83**, 064010, (2011). [http://arxiv.org/abs/1012.2456 [gr-qc]1012.2456 [gr-qc]].

[139] Barausse, Enrico, Buonanno, Alessandra, Hughes, Scott A., Khanna, Gaurav, O'Sullivan, Stephen et al., "Modeling multipolar gravitational-wave emission from small mass-ratio mergers", *Phys.Rev.*, **D85**, 024046, (2012). [http://dx.doi.org/10.1103/PhysRevD.85.024046DOI], [http://arxiv.org/abs/1110.3081arXiv:1110.3081 [gr-qc]].

[140] A. Taracchini *et al.*, "Effective-one-body model for black-hole binaries with generic mass ratios and spins," Phys. Rev. D **89**, no. 6, 061502 (2014) [arXiv:1311.2544 [gr-qc]].

[141] T. Damour and A. Nagar, "New effective-one-body description of coalescing nonprecessing spinning black-hole binaries," Phys. Rev. D **90**, no. 4, 044018 (2014) [arXiv:1406.6913 [gr-qc]].

[142] T. Damour, A. Nagar and S. Bernuzzi, "Improved effective-one-body description of coalescing nonspinning black-hole binaries and its numerical-relativity completion," Phys. Rev. D **87**, 084035 (2013) [arXiv:1212.4357 [gr-qc]].

[143] M. Pürrer, "Frequency domain reduced order models for gravitational waves from aligned-spin compact binaries," Class. Quant. Grav. **31**, no. 19, 195010 (2014) [arXiv:1402.4146 [gr-qc]].

[144] B. P. Abbott *et al.* [LIGO Scientific and Virgo Collaborations], "GW150914: First results from the search for binary black hole coalescence with Advanced LIGO," Phys. Rev. D **93**, no. 12, 122003 (2016) doi:10.1103/PhysRevD.93.122003 [arXiv:1602.03839 [gr-qc]].

[145] P. Ajith *et al.*, "Phenomenological template family for black-hole coalescence waveforms," Class. Quant. Grav. **24**, S689 (2007) [arXiv:0704.3764 [gr-qc]].

[146] M. Hannam, P. Schmidt, A. Boh, L. Haegel, S. Husa, F. Ohme, G. Pratten and M. Prrer, "Simple Model of Complete Precessing Black-Hole-Binary Gravitational Waveforms," Phys. Rev. Lett. **113**, no. 15, 151101 (2014) [arXiv:1308.3271 [gr-qc]].

[147] S. Khan, S. Husa, M. Hannam, F. Ohme, M. Prrer, X. Jimnez Forteza and A. Boh, "Frequency-domain gravitational waves from nonprecessing black-hole binaries. II. A phenomenological model for the advanced detector era," Phys. Rev. D **93**, no. 4, 044007 (2016) [arXiv:1508.07253 [gr-qc]].